

Review

Open Access



Design of Zn anode protection materials for mild aqueous Zn-ion batteries

Yuejuan Zhang^{1,3}, Songshan Bi², Zhiqiang Niu^{2,*}, Weiya Zhou^{1,3,4,5,*}, Sishen Xie^{1,3,4,5,*}

¹Beijing National Research Center for Condensed Matter Physics, and Institute of Physics, Chinese Academy of Sciences, Beijing 100190, China.

²Key Laboratory of Advanced Energy Materials Chemistry (Ministry of Education), Renewable Energy Conversion and Storage Center, Haihe Laboratory of Sustainable Chemical Transformations, College of Chemistry, Nankai University, Tianjin 300071, China.

³School of Physical Sciences, and College of Materials Science and Opto-Electronic Technology, University of Chinese Academy of Sciences, Beijing 100049, China.

⁴Songshan Lake Materials Laboratory, Dongguan, Guangdong 523808, China.

⁵Beijing Key Laboratory for Advanced Functional Materials and Structure Research, Beijing 100190, China.

***Correspondence to:** Prof. Weiya Zhou, Beijing National Research Center for Condensed Matter Physics, and Institute of Physics, Chinese Academy of Sciences, No. 8, 3rd South Street, Zhongguancun, Haidian District, Beijing 100190, China. E-mail: wyzhou@iphy.ac.cn; Prof. Zhiqiang Niu, Key Laboratory of Advanced Energy Materials Chemistry (Ministry of Education), Renewable Energy Conversion and Storage Center, Haihe Laboratory of Sustainable Chemical Transformations, College of Chemistry, Nankai University, No. 94, Weijin Road, Nankai District, Tianjin 300071, China. E-mail: zqniu@nankai.edu.cn; Prof. Sishen Xie, Beijing National Research Center for Condensed Matter Physics, and Institute of Physics, Chinese Academy of Sciences, No. 8, 3rd South Street, Zhongguancun, Haidian District, Beijing 100190, China. E-mail: sxxie@iphy.ac.cn

How to cite this article: Zhang Y, Bi S, Niu Z, Zhou W, Xie S. Design of Zn anode protection materials for mild aqueous Zn-ion batteries. *Energy Mater* 2022;2:200012. <https://dx.doi.org/10.20517/energymater.2022.08>

Received: 8 Mar 2022 **First Decision:** 28 Mar 2022 **Revised:** 11 Apr 2022 **Accepted:** 13 Apr 2022 **Published:** 24 Apr 2022

Academic Editors: Yuping Wu, Wei Tang **Copy Editor:** Tiantian Shi **Production Editor:** Tiantian Shi

Abstract

Rechargeable aqueous Zn-ion batteries (AZIBs) are considered alternative stationary storage systems for large-scale applications due to their high safety, low cost, and high power density. However, Zn anode issues including dendrite formation and side reactions greatly hinder the practical application of AZIBs. To solve the Zn anode issues, various strategies based on material designs have been developed. It is necessary to analyze and classify these strategies according to different materials, because different properties of materials determine the underlying mechanisms. In this review, we briefly introduce the fundamental issues in Zn anodes. Furthermore, this review highlights the material designs for the protection of Zn anodes in mild AZIBs. Finally, we also offer insight into potential directions in the material designs to promote the development of AZIBs in the future.



© The Author(s) 2022. **Open Access** This article is licensed under a Creative Commons Attribution 4.0 International License (<https://creativecommons.org/licenses/by/4.0/>), which permits unrestricted use, sharing, adaptation, distribution and reproduction in any medium or format, for any purpose, even commercially, as long as you give appropriate credit to the original author(s) and the source, provide a link to the Creative Commons license, and indicate if changes were made.



Keywords: Material design, Zn anode protection, aqueous Zn-ion battery, dendrites, hydrogen evolution reaction

INTRODUCTION

Rechargeable aqueous Zn-ion batteries (AZIBs) are regarded as a promising candidate for next-generation energy storage systems due to their remarkable advantages^[1-6]. Common AZIBs are composed of Zn²⁺ storage cathodes, Zn metal anodes, and aqueous electrolytes containing Zn²⁺ salt. Among them, the typical cathode materials can be mainly divided into manganese-based oxides, vanadium-based oxides, Prussian blue analogs, and organic compounds^[7-15]. Mild AZIBs usually refer to the pH range of their electrolytes of ca. 4-6^[16]. There are several advantages of AZIBs. For instance, aqueous batteries are safe, cheap, and can be assembled in air. Moreover, higher ion conductivity can be obtained in aqueous electrolytes than the case in organic electrolytes^[17]. As a result, aqueous batteries often possess high power density^[18]. Besides, compared with alkaline metals and Ca/Mg/Al, Zn has suitable equilibrium electrode potential [-0.76 V vs. standard hydrogen electrode (SHE)] and high hydrogen evolution reaction (HER) overpotential in aqueous electrolytes. As a result, Zn metal can be directly used as the anode in aqueous electrolytes. Furthermore, Zn anodes with two-electron transfer characteristics possess high theoretical capacity (5855 mAh cm⁻³ and 820 mAh g⁻¹), leading to high energy density. These advantages make AZIBs have great prospects in the field of large-scale energy storage systems^[19-20].

The electrochemical performance of AZIBs mainly depends on the design of cathodes and anodes. Normally, Zn metal can directly serve as the anodes in AZIBs. However, Zn anodes suffer from two main issues: dendrite growth and side reactions^[21-23]. Similar to the Li dendrites in lithium-ion batteries^[24-25], the unlimited growth of Zn dendrites on Zn anodes is also a fatal hazard for AZIBs due to the nonuniform Zn nucleation and deposition. The dendrites may pierce the separator and eventually cause the batteries to fail. In addition, the side reactions such as HER, corrosion, and passivation, driven by the contact between Zn anodes and aqueous electrolytes, are also regarded as big threats to AZIBs. The side reactions not only greatly increase the polarization but also reduce the Coulombic efficiency (CE) of the cell. The two issues of Zn anodes exist simultaneously and promote each other, which seriously affects the reversibility of Zn chemistry and the electrochemical performance of AZIBs.

Therefore, some strategies have been developed to stabilize the Zn anodes^[26-29], including surface modification, structural design, and electrolyte regulation, as presented in [Figure 1](#). These strategies effectively suppress the Zn dendrite growth and/or side reactions, thus being beneficial for enhancing the electrochemical performance of AZIBs. However, a comprehensive review of strategies focusing on material designs for stabilizing the Zn anodes is still absent. In this review, we describe the origins and hazards of dendrite formation and side reactions of Zn anodes in mild AZIBs. Subsequently, we focus on the material design strategies for the protection of Zn anodes and the high performance of AZIBs. The characteristics and functions of these materials on Zn anodes are discussed in detail. Finally, the challenges and further prospects of material designs for Zn anodes are put forward.

ZN ANODE ISSUES

In general, Zn metal is directly deployed as the anodes of AZIBs. The AZIBs with Zn metal anodes have great potential for large-scale energy storage due to their safety and low cost. However, their practical performances are still not as good as expected, which are primarily impeded by the anode-electrolyte interface issues. These issues mainly include dendrite formation and side reactions on the surface of Zn anodes and are analyzed as follows.

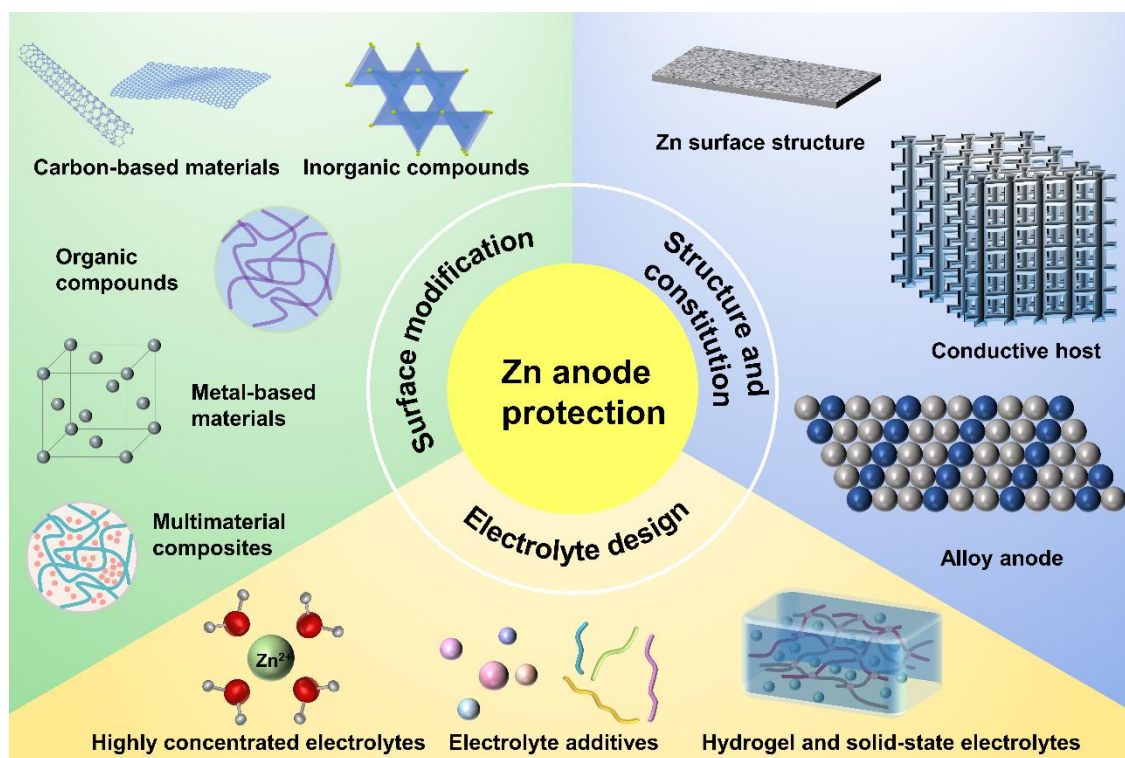


Figure 1. Schematic diagram of the material designs for stabilizing Zn anodes in mild AZIBs.

Dendrite formation

In the mild aqueous electrolyte, the reaction mechanism of a Zn anode can be summarized as follows:



During electrodeposition, Zn^{2+} typically undergoes four processes: adsorption, diffusion, nucleation, and growth. These processes are susceptible to the surface microenvironment of Zn anodes. Specifically, the surface of Zn anodes is not atomically smooth, which could result in uneven electric field distribution, heterogeneous ion flux distribution, and different nucleation barrier sites on Zn anodes. As a result, Zn^{2+} is more likely to adsorb and aggregate on the higher active sites under the unrestricted 2D Zn^{2+} diffusion [Figure 2A]^[30]. Then, the Zn^{2+} would nucleate on these sites to form Zn atomic clusters. The formed Zn atomic clusters disperse heterogeneously on the surface of Zn, which would further exacerbate the uneven field distribution in turn. These clusters can also serve as tiny protrusions with larger curvature and induce Zn dendrite growth due to the tip effect [Figure 2B and C]^[31]. The growing Zn dendrites would bring several hazards. Owing to the loose and porous 3D structure of Zn dendrites, more of the fresh Zn could contact with aqueous electrolytes, leading to more reaction sites for side reactions. In addition, the dendrites are prone to breaking away from Zn substrate and then becoming “dead Zn” due to the bad connection between the dendrites and anodes. The inactive “dead Zn” with the insulating byproduct layer increases the internal resistance and polarization of the battery. In addition to “dead Zn”, some dendrites could continually grow along with the separator until they pierce it and thus cause a short circuit.

Side reactions

In addition to the dendrite growth, other detrimental problems of Zn anodes are side reactions, including HER, corrosion, and passivation. Among them, HER is the primary problem, which is described as follows:

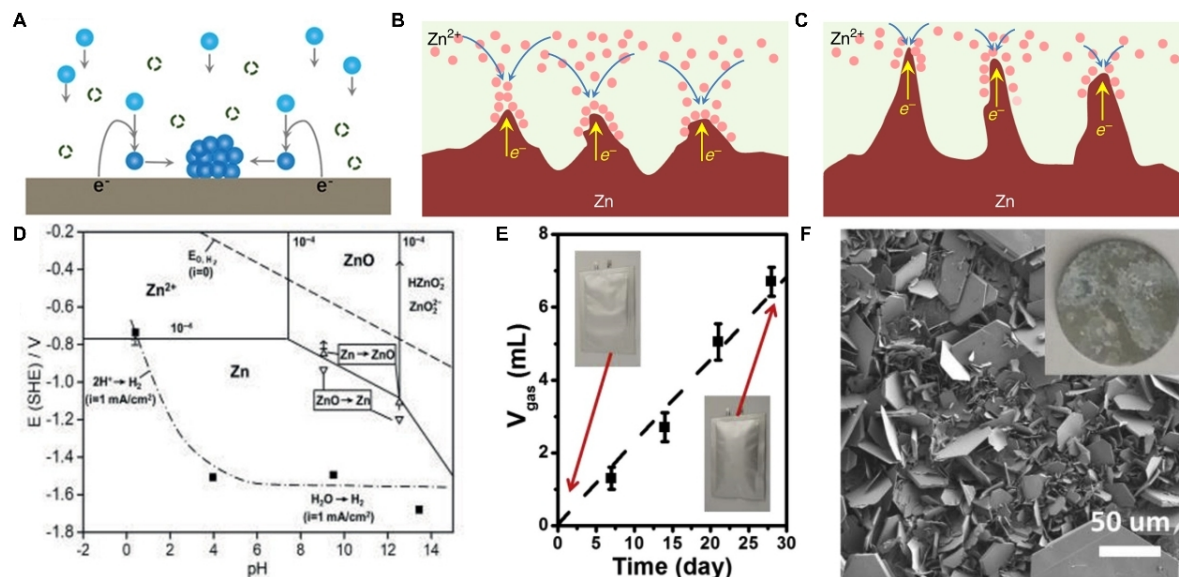


Figure 2. (A) Schematic diagram of Zn atomic clusters formation under unrestricted 2D Zn²⁺ diffusion^[30]. (B) Schematic diagram illustrating the tip effect. (C) The formation of dendrites^[31]. (D) Pourbaix diagram of the Zn/H₂O system containing 10⁻⁴ M Zn²⁺^[32]. (E) The gas evolution of Zn symmetric cell after resting different times in 3 M ZnSO₄ electrolyte. (F) The surface morphology of Zn anode after immersing in 3 M ZnSO₄ electrolyte for 30 days^[33]. Reproduced from Ref.^[30], Ref.^[31], and Refs.^[32-33] with permission from Wiley-VCH, Springer Nature, and Elsevier, respectively.



Specifically, Zn²⁺/Zn has a lower equilibrium potential than that of H₂O/H₂ in the entire pH range, according to the Pourbaix diagram [Figure 2D]^[32]. Therefore, HER tends to occur on Zn metal anode surface by chemical or electrochemical processes due to the thermodynamic activity of Zn in an aqueous solution [Figure 2E]^[33]. As a result, an accompanying Zn corrosion process would exist, and HER competition with the Zn plating would occur during the charging process of AZIBs. HER increases the internal pressure of the battery, which could further cause extremely increased polarization, swell, and even burst the battery. In addition, HER also results in an increased pH at the anode surface due to the accumulated OH⁻. The continuously increased OH⁻ would further react with Zn²⁺ and anion of Zn salts to form byproducts with limited solubility [Figure 2F]^[33], such as Zn(OH)₂, Zn₄SO₄(OH)₆·xH₂O (ZHS), etc. These byproducts are electrical insulators and passivate the Zn surface to block the sites for further Zn plating/stripping. In the meantime, they are loose in the structure; thus, they cannot avoid the further HER and Zn corrosion on the Zn anodes. Therefore, Zn and electrolytes around anodes are constantly consumed, leading to an inferior CE. Moreover, the rough and uneven surface caused by corrosion and passivation could further accelerate the growth of Zn dendrites.

MATERIAL DESIGNS FOR SURFACE MODIFICATION ON ZN METAL

Surface modification on Zn metal is recognized as an attractive and effective strategy to solve the serious issues on Zn anode-electrolyte interfaces, such as dendrite growth and side reactions. Surface modified layers can be obtained through doctor-blade coating, pre-reaction, physical vapor deposition (such as magnetron sputtering, ion beam sputtering, and thermal evaporation), chemical vapor deposition [CVD, such as atomic layer deposition (ALD)], etc. In general, the modified layers have two functions: (1) as a barrier layer to isolate the Zn anodes from the water of aqueous electrolytes; and (2) as a guiding layer to

assist the uniform Zn deposition. To realize their functions, the ideal modified layers need to meet the following requirements: (1) high Zn^{2+} conductivity, facilitating fast ion diffusion and good deposition kinetics; (2) high adhesion to the Zn surface, high mechanical stability, and high dynamic adaptability, ensuring effective protection of Zn under the dramatic volume changes while Zn plating/stripping; (3) light weight and thin thickness, avoiding the remarkable degradation of energy and power densities of the batteries; and (4) cheap materials and simple preparation process. Many materials have been used as Zn surface modification thus far, which can be classified into carbon-based materials, inorganic compounds, organic compounds, metal-based materials, and composite materials.

Carbon-based materials

Carbon materials with outstanding electrical conductivity have been extensively utilized as modified layers of Zn anodes to inhibit the formation of Zn dendrites in AZIBs. As described above, under an uneven electric field, Zn dendrites are inclined to form on the anodes. The high electrical conductivity and large specific surface area of carbon materials are beneficial to uniform the interfacial electric field distribution and avoid charge accumulation on the Zn anode surface, thus effectively avoiding dendrite proliferation and stabilizing the Zn anodes. Commercially available carbon materials (activated carbon^[34], graphite^[35], *etc.*) with convenient manufacturing processes can be directly assembled on the anode surface to protect the Zn anodes. For example, Du *et al.*^[36] mixed carbon fibers, acetylene black, and polyvinylidene fluoride (PVDF) to prepare a slurry, which was then sprayed onto the surface of Zn foil to form a carbon fiber micron film (CFMF) [Figure 3A]. By virtue of its high conductivity and surface area, CFMF could improve Zn electrodeposition kinetics and homogenize the electrical field. The porous scaffold structure of CFMF could also accommodate the Zn anode volume changes during cycling, thus endowing a stable cycling performance of 2500 h at 1 mA cm^{-2} and 1 mAh cm^{-2} in the symmetric cells^[36]. It is worth noting that such a strategy could be extended to Li metal anodes for inducing the enhanced electrochemical performance^[36].

Compared with commercial carbon materials, carbon nanomaterials have received more attention since they can adjust the Zn deposition by their larger specific surface area and nanoscale size. The common carbon nanomaterials that are utilized in protecting Zn anodes mainly include CNT^[37], graphene^[38-40], mesoporous hollow carbon spheres^[41], and various other carbon nanomaterials^[42-44]. In particular, graphene-based materials usually exhibit a small lattice misfit (no larger than 25% as an empirical value) with Zn (002); thus, they can induce reversible lamella-nanostructured Zn (002) epitaxial electrodeposition, which presents a non-dendritic Zn deposition^[38,45]. Inspired by this, Zhang *et al.*^[46] designed a cellulose nanowhisker-graphene (CNG) membrane on a Zn anode surface. The CNG membrane induced a redirected Zn (0002) deposition due to the graphene component. Moreover, the CNG could restrain the contact between Zn anode and water molecules through an enhanced $[\text{Zn}(\text{H}_2\text{O})_6]^{2+}$ desolvation process, which alleviated HER and Zn corrosion. Simultaneously, the CNG could shield anions due to the deanionization shock from surface negative charges. Therefore, the inert byproducts were effectively inhibited. Benefitting from the suppressed Zn dendrites and side reactions, the CNG-modified Zn anodes achieved stable cycles for 5500 h at 0.25 mA cm^{-2} and 0.5 mAh cm^{-2} . In addition to modifying the Zn anode surface, graphene-based materials can also be utilized on separators to stabilize the Zn anodes^[47-48]. For instance, a vertical graphene (VG) carpet^[49] growing on one side of separators could effectively homogenize the current distribution, smooth the electric field distribution, and lower the local current density [Figure 3B]. Therefore, it can regulate Zn^{2+} transport behavior and induce a dendrite-free deposition. Furthermore, when mixing graphene-based materials with other materials to serve as separators, regulated (002) Zn deposition behavior can also be achieved. Inspired by this, Cao *et al.*^[50] designed a cellulose/GO (CG) composite separator. Benefitting from the in-plane and dendrite-free Zn deposition [Figure 3C], the CG induced stable cycles for 1750 h at 2 mA cm^{-2} and 1 mAh cm^{-2} , which was far more than the 35 h achieved by the commercial glass fiber separator [Figure 3D]. In addition to the regulation of the electric

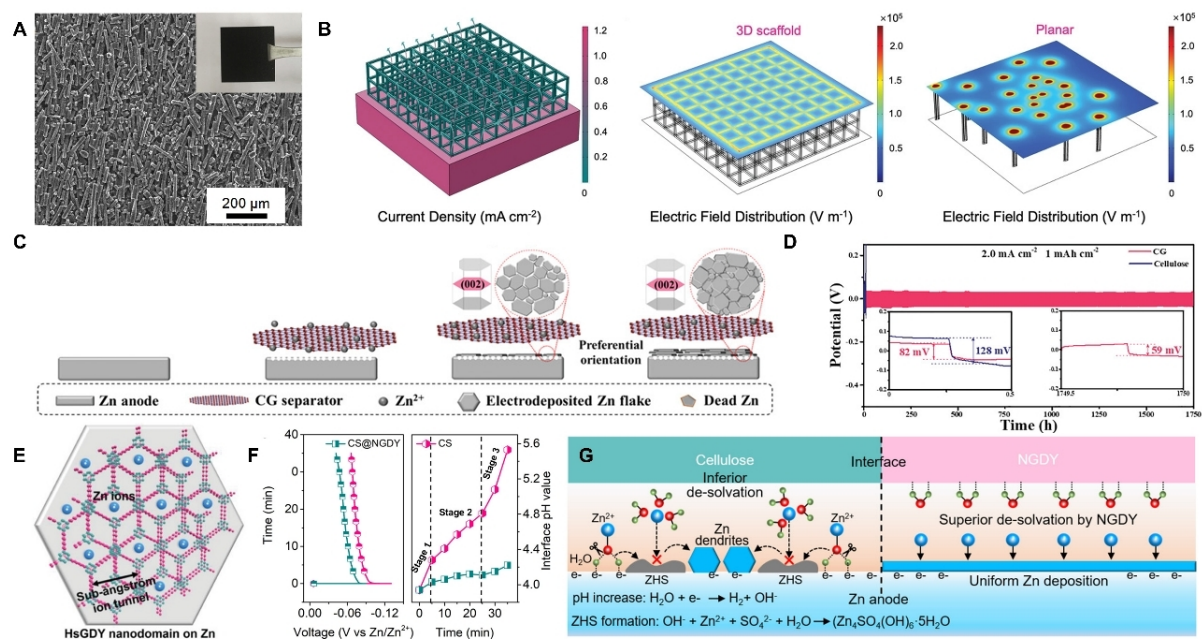


Figure 3. (A) Surface morphology of CFMF coated on Zn anode surface^[36]. (B) Current distribution and electric field distribution of separator with VG (3D scaffold), and electric field distribution of pristine separator (2D planar structure)^[49]. (C) Schematic diagram of CG separator inducing preferential orientation deposition of Zn. (D) The galvanostatic charge/discharge profile of Zn symmetric cells with CG or cellulose separator^[50]. (E) Schematic illustration of the sub-Ångström ion tunnel of HsGDY^[55]. (F) The effect of different separators on interface pH change around Zn anode. (G) Schematic diagram illustrating stabilization of interface pH and suppression of Zn dendrites using the CS@NGDY^[56]. Reproduced from Ref.^[36] and Refs.^[49-50,55-56] with permission from Wiley-VCH and Elsevier, respectively.

field and Zn^{2+} ions, some functionalized carbon-based materials can offer lots of zincophilic active sites for Zn nucleation and deposition^[51]. These sites could capture and redistribute the Zn^{2+} and result in lower nucleation overpotential, which is also conducive to dendrite-free Zn deposition.

Graphdiyne is also a typical 2D carbon material similar to graphene^[52-54]. Graphdiyne can redistribute Zn^{2+} concentration field through special ion tunnels. For instance, Yang *et al.*^[55] synthesized hydrogen-substituted graphdiyne (HsGDY) as Zn surface protection by in situ growth. They found that HsGDY could promote a homogeneously dispersed Zn^{2+} around the Zn surface, benefitting from its sub-Ångström level ion tunnels [Figure 3E]. Based on HsGDY, the modified Zn exhibited a long lifetime over 2400 h in symmetric cells and stable 10,000 cycles in the full batteries coupled with a high 22.95 mg cm^{-2} loading mass of N-doped porous carbon cathode. Furthermore, they also found that a stable Zn-electrolyte interface could be obtained when the graphdiyne was used to modify the separators. To confirm this, an N-modification graphdiyne interface (NGDY) on a cellulose separator (CS@NGDY) was constructed^[56]. NGDY could stabilize interface pH by accelerating the desolvation process of hydrated Zn^{2+} [Figure 3F]. This could be explained by the fact that the N atoms of NGDY would interact with coordinated H_2O of hydrated Zn^{2+} and capture electrons from the coordinated H_2O [Figure 3G], which would further reduce activation energy and avoid the weakening of O-H bonds. Therefore, the CS@NGDY suppressed HER and the formation of ZHS, increasing the lifespan of symmetric cells by 116 times at 10 mA cm^{-2} and 1 mA h cm^{-2} .

Inorganic compounds

Inorganic compounds usually have excellent electrochemically and chemical stability in mild electrolytes. As a result, they can serve as a stable barrier layer to isolate the Zn metal to form bulky electrolytes, which is conducive to mitigating the HER and Zn corrosion. Various inorganic compounds have been reported as Zn anode coating materials so far, such as metal oxides, metal sulfides, metal nitrides, inorganic salts, MXene, etc.

Metal oxides have been broadly utilized to inhibit dendrites and side reactions. Different metal oxides possess different properties; thus, they can affect the Zn anode-electrolyte interface in various ways when they decorate the Zn anode surface. For example, ZrO_2 ^[57-58] and Sc_2O_3 ^[59] have a high dielectric constant. When they are used as coating layers to modify the anode-electrolyte interface, they can induce controllable nucleation sites for Zn^{2+} as well as fast Zn^{2+} transport due to the Maxwell-Wagner polarization between the Zn anodes and the layers. In addition, Al-doped ZnO (AZO) prepared by magnetron sputtering possesses strong adsorption energy to Zn^{2+} due to the doped Al [Figure 4A]^[60]. Therefore, AZO can provide abundant sites to attract Zn^{2+} , facilitating the desolvation of hydrated Zn^{2+} and regulating the Zn^{2+} flux [Figure 4B]. It is noteworthy that a coating with low Zn affinity can also adjust the Zn^{2+} flux. Because of its relatively low Zn affinity [Figure 4C], the F-TiO₂ protective layer with a highly exposed (001) facet can repulse Zn^{2+} to the Zn-layer interface [Figure 4D], thus leading to increased interfacial Zn^{2+} concentration and the subsequent uniform nucleation and lateral growth^[61]. Moreover, some metal oxides (TiO₂ (4.4-5.0 eV), WO₃ (4.3-4.8 eV), MoO₃ (6.2-6.7 eV), and CeO₂ (4.3-4.7 eV)) have a higher work function than Zn (3.6-3.8 eV), which means that the electrons can flow from Zn to the metal oxide to build an Ohmic contact interface when using these metal oxides as Zn anode protective layers [Figure 4E]^[62]. The Ohmic contact interface would further induce an anti-blocking layer at the interfaced metal oxides [Figure 4E]. The anti-blocking layer can not only improve Zn^{2+} diffusion but also reduce the Zn^{2+} nucleation barrier, thus regulating the homogeneous Zn deposition behavior. In addition to the inherent properties, a 3D nanoporous structure of ZnO can also accelerate the desolvation of hydrated Zn^{2+} and thus relieve the side reactions^[63]. However, most metal oxides have good surface wettability. When the metal oxides layers have a large pore structure^[64-65], the layers cannot completely inhibit the HER despite their effective suppression for Zn dendrites. Therefore, entire coverage and conformal deposition techniques are needed and should be considered, such as ALD^[66-67].

In addition to metal oxides, other metal compounds have also been designed as protective layers of the Zn surface, such as sulfides (ZnS ^[68] and MoS_2 ^[69]), nitrides (N-Zn^[70], TiN^[71], and Cu_3N ^[72]), fluorides (ZnF_2 ^[73-75] and gradient fluorinated alloy^[76]), phosphides (ZnP ^[77] and ZrP ^[78]), etc. These metal compounds contain S, N, F, or P atoms that exhibit a good affinity for Zn. Therefore, they can redistribute the Zn^{2+} flux, drive fast Zn^{2+} diffusion, and tightly adhere to the Zn anode surface. For instance, S atoms could bond with the Zn atoms at the Zn metal and ZnS interphase, which would induce an unbalanced charge distribution [Figure 4F] and further accelerate the Zn^{2+} diffusion through ZnS layer^[68]. Moreover, a ZnS layer with poor electronic conductivity was in situ obtained on the Zn anodes by a vapor-solid strategy. Therefore, the ZnS layer was dense and robust, which exhibited good suppression for Zn dendrite growth and side reactions^[68]. In addition to inhibiting the Zn dendrite, the metal compounds can also regulate the growth pattern of the byproduct through tuning their specific orientations. Taking TiN as an example, the (200) crystal facet of TiN on Zn anode was conducive for parallel ZHS, while the (111) one could lead to the vertical growth of ZHS [Figure 4G]^[71]. By virtue of uniform Zn deposition and alleviated side reaction, these metal compounds exhibit excellent cycle stability even under harsh conditions. For instance, a ZnP layer was designed on the Zn surface using electrodeposition. The ZnP layer could induce stable symmetric cells with over 100 h cycling at a large depth of discharge (DOD ~ 82%, 48 mAh cm⁻²) and a high current density of 15 mA cm⁻²^[77]. In addition, a ZnF_2 layer formed on the Zn anodes via an in situ ion metathesis method possessed a high

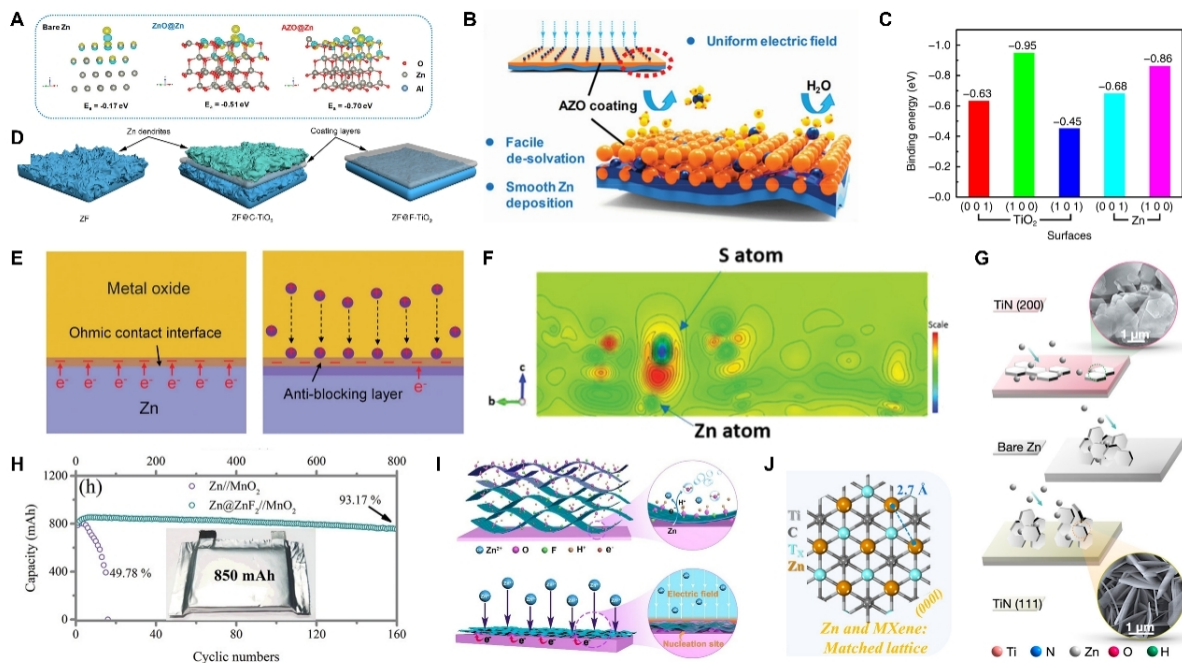


Figure 4. (A) Binding energies of a foreign Zn²⁺ with the surfaces of bare Zn, ZnO coating, and AZO coating. (B) Schematic illustrating the effect of AZO coating on Zn deposition process^[60]. (C) Binding energies between Zn atom and different facets of TiO₂ and Zn. (D) Schematic illustration of the Zn plating process on Zn foil (ZF), commercial TiO₂-coated ZF (ZF@C-TiO₂), and faceted TiO₂-coated ZF (ZF@F-TiO₂)^[61]. (E) Schematic diagram of the formation of an Ohmic contact interface and the anti-blocking layer^[62]. (F) The slice of the electron density difference map illustrating the unbalanced charge distribution^[68]. (G) Effect of different facets of TiN on the growth pattern of byproduct^[71]. (H) Cycling stability of AZIBs with 850 mAh at 0.2 C^[73]. (I) Self-assembly process of MXene layer on the Zn anode surface and the regulation of MXene layer on Zn deposition^[90]. (J) Schematic illustrating the lattice matching degree between Zn anode and MXene^[92]. Reproduced from Refs.^[60,62,68,73,90], Ref.^[61], and Refs.^[71,92] with permission from Wiley-VCH, Springer Nature, and American Chemical Society, respectively.

Zn²⁺ transfer number of 0.65^[73]. Based on the ZnF₂ layer, an 850 mAh large-capacity battery was successfully obtained coupled with the MnO₂ cathode. This battery could achieve 160 cycles with 93.17% capacity retention at 0.2 C [Figure 4H]^[73].

Inorganic salts have also been widely researched as modified materials on Zn anode surface. Some inorganic salts can act as fast Zn²⁺ conductors to facilitate Zn²⁺ diffusion at the interface between the anode and electrolyte, such as Zn-Mont^[79], Mg-Al layered double hydroxide^[80], NaTi₂(PO₄)₃^[81], *etc.* Usually, these inorganic salts possess large interlayer space^[82] or voids^[81], which can serve as Zn²⁺ channels or sites to lower Zn²⁺ migration barrier. Therefore, they can guarantee rapid Zn²⁺ transfer kinetics and regulate Zn²⁺ flux. Moreover, these inorganic salts can function as an inert shield to prevent electron tunneling. As a result, they can eliminate Zn dendrites and side reactions simultaneously. In addition, some inorganic salts have similar characteristics as metal oxides^[83]. BaTiO₃ (BTO), for instance, has a giant dielectric constant. When coated on the Zn surface, the BTO layer would induce an additional directional electric field on the Zn surface under an external field, thus regulating the interfacial electric field and further rendering an ordered and fast Zn²⁺ migration^[84-85]. Furthermore, some metal salts can also offer abundant sites for the Zn²⁺ adsorption to induce uniform Zn nucleation and deposition, such as O-atom sites in ZnMoO₄^[86] and metal sites in NiCo layered double hydroxides^[87].

As a kind of 2D transition metal carbides/nitrides^[88-89], MXene is an attractive candidate for Zn anode protection. Owing to the good electrical conductivity, abundant surface functional groups (-OH, -O, and -F) and hydrophilicity, MXene can induce uniformly distributed electric field and Zn²⁺ flux when it is constructed on the Zn anode surface. Similar to rGO^[40], MXene could be in situ assembled on the Zn surface [Figure 4I]^[90-91]. The in situ formed MXene layer had a tight combination with the Zn anodes, which was beneficial for fast Zn²⁺ transport and low Zn nucleation barrier. As a result, the MXene layer could induce a dendrite-free morphology and even a preferentially oriented Zn deposition. In addition, the surficial terminations of MXene have a significant influence on the Zn²⁺ deposition. Recently, Li *et al.*^[92] studied Mxenes with different halogen functional groups (-Cl₂, -Br₂, and -I₂) as Zn surface modified layers via changing the etchant. They found that halogen surficial termination could tune the Zn²⁺ distribution to tile the Zn²⁺ on the MXene substrate. Especially, the Cl termination could better regulate the Zn²⁺ than O/F, Br, and I due to its moderate Zn²⁺ adsorption and diffusion coefficient. Moreover, Ti₃C₂ matrix had high lattice matching (90%) with Zn [Figure 4J] and thus could induce Zn to deposit along the (0001) crystal plane^[92]. With the synergetic effect, the modified Zn presented over 9000 cycles at 3 A g⁻¹ in the full battery coupled with the Ti₃C₂I₂ cathode^[92].

Organic compounds

Unlike rigid inorganic compounds oxides, organic compounds, especially polymers, usually exhibit better flexibility to accommodate the large volume changes during cycles. More importantly, organic compounds have abundant and changeable functional groups, making their properties easy to regulate. The organic compounds designed for Zn anode modification mainly contain polymers and metal-organic frameworks (MOFs).

Polymers possess abundant polar functional groups and have been extensively studied to protect Zn anodes. The polymers have several functions: (1) serve as an ion regulator to Zn²⁺ migration through the adsorption or coordination of the functional groups^[93], further redistributing the Zn²⁺ flux field and restricting Zn²⁺ 2D diffusion; (2) act as an electrostatic shield^[94] to avoid Zn²⁺/electron aggregation and eliminate tip effects, thus suppressing the growth of Zn dendrites; and (3) function as a desolvation shield^[95-96] or physical barrier layer^[97-99] to reduce water molecules on the Zn surface, further inhibiting the side reactions and HER. It is worth mentioning that some polymers (such as PVDF^[100] and its copolymers^[101]) are ferroelectric materials and can regulate Zn²⁺ transport just as BTO discussed above does when they are coated on the surface of Zn anodes. At present, many polymers have been studied as the Zn anode surface modification, including PA^[102-103], PAM/PVP^[94], polymer glue^[97,104], polysiloxane^[105], PPy^[106], PAN^[107], polystyrene^[99], g-C₃N₄^[108], COFs^[109-111], COPs-CMC^[112], PI^[113], gelatin^[114], *etc.* Due to the advantages discussed above, polymers can induce improved electrochemical performance of Zn anodes. For instance, Zhao *et al.*^[102] proposed a PA coating layer on Zn anode surface inspired by the brightener. The PA layer extended the lifespan of Zn anodes from 131 to 8000 h at 0.5 mA cm⁻² and 0.25 mAh cm⁻². This could be attributed to two points. First, PA possessed rich polar amide groups in its molecules. These groups could strongly coordinate with Zn²⁺ and form a unique H-bonding network. The strong interactions between PA and Zn²⁺ could alter the Zn²⁺ distribution and restrict Zn²⁺ 2D diffusion, which eventually led to uniform Zn deposition. The formed H-bonding network could constrain the water molecules to form solvated Zn²⁺, thus decreasing the water content on the Zn surface^[102]. Second, the PA layer could directly block the water/oxygen to form bulky electrolytes to suppress the detrimental side reactions.

MOFs have also attracted great attention in recent investigations as surface modification materials for their adjustable pores and non-conduction. The porous structure of MOFs can significantly regulate the Zn²⁺ transport dynamics around the surface of Zn anodes. For instance, Liu *et al.*^[115] explored the possibility of UIO-66 MOFs as modified materials on Zn metals. The microporous structure of MOFs facilitated a

hydrophilic interface and a nano-level wetting effect with Zn [Figure 5A], which further adjusted the Zn^{2+} flux on the Zn anodes and induced a non-dendrite Zn deposition. Moreover, MOFs can serve as molecule sieves to block active water molecules from reaching the active sites. Yang *et al.*^[116] developed a ZIF-7 coating to form a super-saturated electrolyte front surface on the Zn anodes [Figure 5B]. They found that the channel structure of the ZIF-7 could repel large-sized solvated Zn^{2+} complexes and partially desolvate the complex in advance under an electric field. Benefitting from this, a changed solvated structure and concentrated electrolyte were obtained in the channel, which further led to a homogeneous Zn deposition and decreased byproduct formation. In addition to the two merits discussed above, MOFs can also induce an electrokinetic effect [Figure 5C]^[117], leading to uniform shock electrodeposition. In the channel of ZIF-11, there were abundant zincophilic functional groups adsorbing the Zn^{2+} , which contributed to forming an EDL. Under an applied electric field, electrokinetic effects such as electro-osmosis, electrophoresis, and surface conduction generated by the EDL^[118] could guide the ZIF-11 with an even Zn^{2+} distribution and a uniform Zn deposition. As a result, the ZIF-11@Cu-Zn-based symmetric cells exhibited increased reversibility and could achieve a stable cycle for 1800 h at 0.5 mA cm^{-2} and 0.25 mAh cm^{-2} ^[117].

Researchers have found that the organic compounds applied to the separators presented similar and beneficial functions because of the meaningful zincophilic functional groups and tunable structure. First, directly employing polymers with zincophilic functional groups as separators is an effective method for stable Zn anodes. Nafion possesses $-\text{SO}_3^-$ groups on its side chains, where the $-\text{SO}_3^-$ groups can interact with Zn^{2+} . As a result, the Nafion membrane separators formed by the casting method could function as a cation selective separator to guide planar ZHS SEI and Zn (002) deposition on the anodes^[119]. Moreover, a Zn^{2+} -substituted Nafion separator could simultaneously induce a uniform electrical field and Zn^{2+} concentration field due to the Donnan potential on the interface^[120]. In addition to the $-\text{SO}_3^-$ groups in Nafion, the $-\text{CN}$ in PAN can also coordinate with Zn^{2+} and thus homogenize the Zn^{2+} distribution. The PAN could guide a preferred Zn (101) deposition when it was used as a nanofiber porous separator via the electrospinning method^[121]. When introducing the Li_2S_3 into the PAN solution, the PAN would react with the Li_2S_3 to form added S-containing functional groups. The added groups would further result in selective Zn^{2+} transport^[122]. Another significant method is to apply the organic compounds to modify the separators. The polymers used on the separator modification include collagen hydrolysate^[123], $g\text{-C}_3\text{N}_4$ ^[124], supramolecules^[125], *etc.* These polymers own abundant zincophilic sites; thus, they can further inhibit the Zn^{2+} accumulation and result in a uniform Zn^{2+} distribution. In addition to polymers, the MOFs can also modify the separators. Benefitting from special ion tunnels in MOFs, the MOF-decorated separators can regulate uniform Zn^{2+} flux^[126] and regulate the solvation structure of Zn^{2+} ^[127]. Therefore, the MOF-modified separators can suppress dendrite formation and side reactions.

Metal-based materials

Metal-based materials often possess good Zn affinity and high conductivity. When they are used as Zn anode protective layers, they can not only provide nucleation sites for Zn deposition but also redistribute the electric field and Zn^{2+} flux on the anode surface^[128-130]. Various metal-based materials have been used to modify Zn metal surface thus far. For instance, $\text{Ni}_5\text{Zn}_{21}$ was designed on the Zn anode surface via electrodeposition^[131]. The $\text{Ni}_5\text{Zn}_{21}$ layer could more strongly bond with Zn atom compared to the bare Zn. Therefore, Zn preferentially nucleated around $\text{Ni}_5\text{Zn}_{21}$, further inhabiting the rambling dendrites growing on the Zn anodes. When the metal-based materials are nanoparticles and uniformly dispersed on the anode surface, they can also act as nanoscale “tips”. These tips have high curvature; thus, they can enlarge the local electric field to strongly attract Zn^{2+} and suppress the large Zn dendrite growth. Based on this, Cui *et al.*^[132] constructed nano-Au particles (NA) on Zn anode surface via sputtering. The size of NA was about 100 nm, and these NA could serve as heterogeneous seeds [Figure 5D]. As a result, the NA decorated anodes achieved uniform Zn-flake-arrays deposition and an enhanced lifespan of 2000 h^[132]. However, Au is

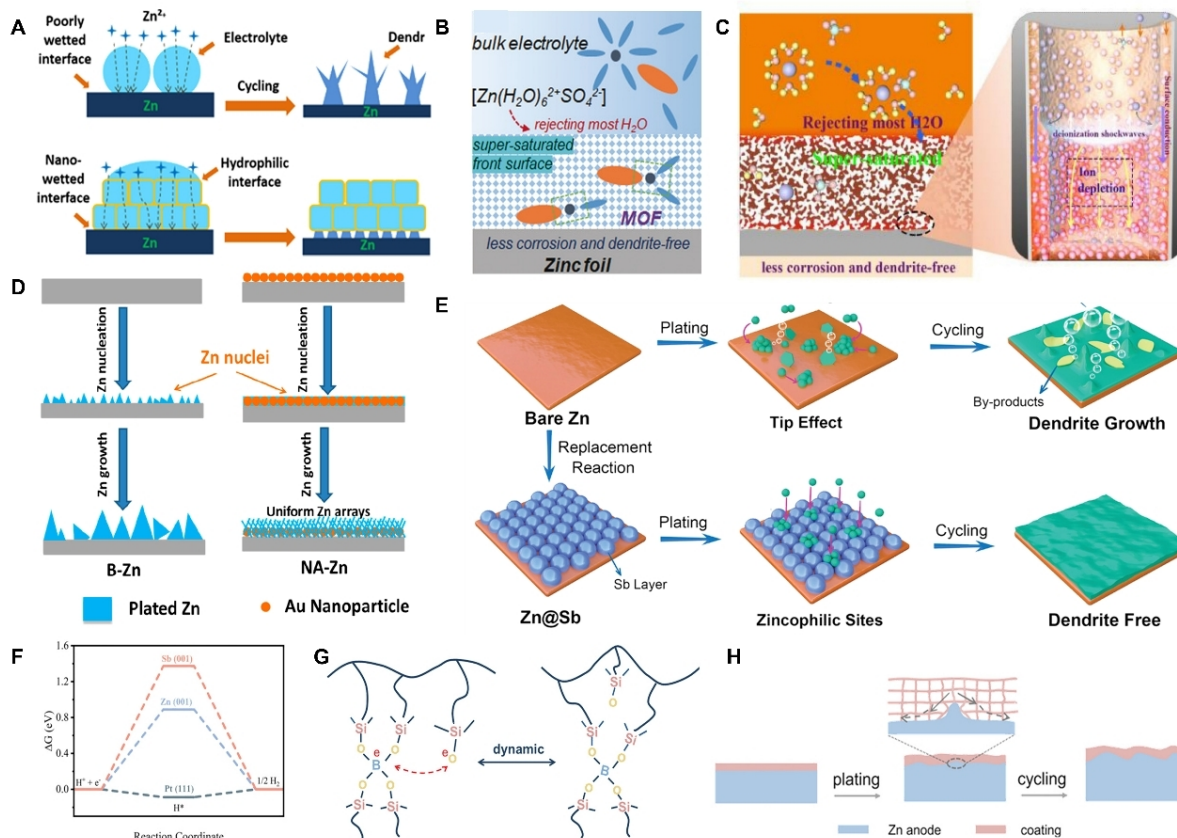


Figure 5. (A) Schematic diagram of Zn anode–electrolyte interface without or with UIO-66 MOFs layer^[115]. (B) Schematic illustrating the formation of super-saturated front surface on the Zn anode by MOF layer^[116]. (C) Schematic diagram of the electrokinetic effect in the MOF layer^[117]. (D) Schematic illustrating the uniform Zn deposition by Au nanoparticle^[132]. (E) Schematic illustration of the Zn plating process on bare Zn and Sb layer modified Zn anode. (F) The H adsorption Gibbs free energy of Sb (001) and Zn (001)^[137]. (G) Schematic illustrating the dynamic micro-crosslinking of B–O bond. (H) The dynamic adaptability of PDMS/TiO_{2-x} layer on the Zn anode surface^[153]. Reproduced from Refs.^[115,132], Refs.^[116,137,153], and Ref.^[117] with permission from American Chemical Society, Wiley-VCH, and Elsevier, respectively.

expensive, and the effect of NA on rampant side reactions should be further explored.

Multifunctional metal-based protective layers on Zn anodes have been extensively developed^[133]. They can not only regulate the uniform Zn deposition but also restrain the side reactions. In has been studied for its higher equilibrium electrode potential (-0.338 V vs. SHE) than Zn and high hydrogen evolution overpotential^[134–135]. Therefore, In can in situ form on Zn surface by cation replacement reaction to inhibit the Zn corrosion and other side reactions^[134–136]. In also possesses a higher Zn atoms adsorption energy than Zn substrate to guide Zn deposition preferentially on the In layer^[135]. Similarly, an Sb metal layer was synthesized on Zn surface by replacement reaction very recently^[137]. The Sb layer could provide abundant zincophilic sites for Zn nucleation and guide uniform Zn²⁺ deposition [Figure 5E]. Meanwhile, it could also homogenize the electric field distribution to avoid the dendrites' formation. Moreover, the Sb metal had a higher H adsorption Gibbs free energy (ΔG_H^{*}) than Zn [Figure 5F]^[137], which indicated that the layer on Zn anodes could suppress the HER process. In addition to In and Sb, Cu^[33], Ag^[138–140], and liquid Ga–In alloy^[141–143] are electrochemical-inert. When they are assembled on Zn anode surface, they can also decrease the side reactions due to their good anticorrosion ability. As discussed above, different metals have slightly different properties when they are used as Zn protective layers. For instance, Ag^[138–140] and Cu^[133,138,144–145]

usually have high Zn affinity; thus, the Ag and Cu metal in protective layers can usually transform into a certain amount of alloy with Zn under cycling, which could further guide the uniform Zn deposition. Sn is not likely to form alloy phases with Zn^[146-147], but Sn is conducive to inhibiting byproduct growth^[148]. To better utilize the properties of different metals, a layer-by-layer anode (Sn/Cu/Zn) was constructed by Huang *et al.*^[148] for long-life AZIBs.

Multimaterial composites

Multimaterial composites, such as organic-inorganic composites and inorganic-carbon composites, usually possess multifunctional and synergistic effects because they can inherit the merits of each ingredient. Therefore, they have been regarded as powerful and promising candidates for Zn anode protection recently. At present, series of organic-inorganic composites have been proposed as protective coatings to protect the Zn anodes, such as PVDF-TiO₂^[149], Nafion-Zn-X^[150], alucone^[151], PAN-Si₃N₄^[152], PDMS/TiO_{2-x}^[153], Zn₃(PO₄)₂-ZnF₂-ZnS with organic outer layer^[154], ZnF₂/Zn₃(PO₄)₂/CF_x^[155], *etc.* These organic-inorganic composites are obtained via mixing two different kinds of matrix to coat the anodes^[149] or in situ built on the Zn anode surface by pre-cycling in organic electrolyte^[154]. In general, the organic (polymer) matrixes have rich functional groups^[150], excellent mechanical flexibility^[149,152] and high dynamic adaptability^[153]. Therefore, they can serve as an elastic constraint to relieve the side reactions. Additionally, the inorganic ingredients in composites can modulate the ion distribution^[156], which would further tune the uniform Zn deposition. For example, the PDMS/TiO_{2-x}^[153] layer was designed by coating a slurry composed of PDMS and TiO_{2-x} on the surface of the Zn plate. The PDMS/TiO_{2-x} layer could adapt to the volume change of Zn anodes during cycles due to the dynamic micro-crosslinking of B-O bond in PDMS [Figure 5G and H]. Moreover, TiO_{2-x} could induce rapid Zn²⁺ transport and uniform Zn deposition. Consequently, the PDMS/TiO_{2-x}-coated anode could achieve stable cycles for 300 h at 10 mA cm⁻² and 10 mAh cm⁻² in symmetry cells^[153].

In addition to the organic-inorganic composites, other composites are also studied as Zn surface protection layers recently, such as Zn₄SO₄(OH)₆·5H₂O/Cu₂O^[157], ZnF₂-Cu^[158], *etc.* These composites can simultaneously promote uniform Zn²⁺ deposition and inhibit side reactions on the Zn surface. Similar to organic-inorganic composites, these composite coatings also inherit the advantages of different materials. For instance, in the S/MXene@ZnS composite layer^[159], doped S could facilitate the electrolyte to penetrate into the Zn anode surface. MXene could effectively homogenize electric field distribution and decrease local current density. Meanwhile, the ZnS could inhibit side reactions, promote uniform Zn²⁺ distribution, and accelerate Zn²⁺ migration. As a result, S/MXene@ZnS induced stable cycles for 1600 h at 0.5 mA cm⁻² and 0.5 mAh cm⁻² in symmetric cells^[159]. Taking the ZnO/C hybrid layer^[160] as another example, the hybrid layer had different advantages, eventually leading to a dendrite-free Zn deposition and suppressed HER: (1) ZnO featured a unique dielectric constant, which could induce controllable Zn²⁺ nucleation and deposition sites; and (2) carbon materials could help to avoid the charge accumulation and buffer structure change during cycling. Benefitting from their merits, the ZnO/C coated Zn symmetric cells achieved stable cycles over 2000 h at 0.25 mA cm⁻² and 0.25 mAh cm⁻²^[160].

MATERIAL DESIGNS OF THE STRUCTURE AND CONSTITUTION OF ZN ANODES

The structure and constitution of anodes play an extremely important role in the localized ion concentration distribution and localized current density^[161-162], thus significantly affecting the local Zn plating/stripping process. Different structures and constitutions of anodes can be obtained by etching, rolling, 3D printing, template method, CVD, freeze-drying, melting method, electroplate, *etc.* In this section, Zn surface structure designs, conductive host designs, and alloy anodes for Zn anode protection are discussed.

Zn surface structure designs

At present, AZIBs primarily use commercial Zn metal as anodes, which has crystal heterogeneity and usually suffers from Zn dendrites with an uneven surface electric field. To regulate Zn deposition, the surface structure designs of Zn anodes have aroused researchers' interest. Special surface structures can be prepared via treating the Zn metal, which can effectively redistribute the electric field evenly for uniform Zn deposition. For instance, 3D ridge-like structure^[163], pitted texture^[164], hexagonal-hole patterns^[165], porous surface architectures^[166], *etc.* can be formed on the surface of the Zn foil just by a simple chemical polishing. It can be attributed to the selective etching of weak crystallographic planes and grain boundaries of Zn. In addition, the surface texture and surficial atomic structure of Zn anodes play significant roles in solving the dendrite problem and improving electrochemical performance. Usually, Zn (002) crystal planes exhibit non-dendrites, non-byproducts, and weak HER in sharp contrast to the other crystal plane^[165]. Therefore, many strategies have been designed to form a preferred (002) crystal plane on the Zn surface, such as an organic acid-etching approach^[167], a large rolling deformation process^[168-169], and a thermal annealing process^[170]. The (002)-textured Zn anode exhibits better electrochemical performance than commercial Zn. For instance, the Zn anodes with preferred (002) orientation formed after accumulative roll bonding (ARB) could achieve hundreds of cycles at 40 mA cm⁻² and 4 mAh cm⁻² in symmetric cells [Figure 6A and B]. By contrast, the pristine Zn anodes failed after only the initial cycles^[169]. Nevertheless, the Zn metal anodes after surface designs cannot avoid the dramatic volume deformation, which might not be conducive to the working conditions of the large DOD and large area current.

Conductive host designs

To accommodate large volume changes of the Zn anodes, more researchers have focused on the host designs of the anodes. The hosts for Zn anodes mainly include metal-based, carbon-based, and MXene hosts. In addition to providing enough space for Zn deposition, the 3D hosts often possess large specific surface areas to cause sufficient contact area. As a result, the 3D hosts can effectively reduce the local current density and simultaneously provide more sites for Zn deposition, which will further inhibit the growth of dendrites.

3D metal-based materials are regarded as popular Zn anode hosts due to their good structure stability and Zn affinity. Zn metal can directly function as the skeleton by designing its 3D structure^[171]. 3D-structure Zn metal anodes can induce spatial selective deposition and thus inhibit the dendrite growth^[172]. Moreover, they can also achieve an interface-localized concentrated electrolyte due to the space charge effect^[173], which is beneficial to suppress the side reactions. Even so, 3D-structure Zn metal anodes still act as both the active material and collector, which could reduce the utilization of Zn. To increase the Zn utilization, non-Zn metal-based hosts have received more attention, such as 3D Cu^[174-176], 3D Ti^[177], *etc.* Taking Ni host as an example, a 3D Ni host with multi-channel lattice structures was prepared using 3D printing and electroless plating techniques recently [Figure 6C]^[178]. Due to the ability to redistribute localized electric field and its super-hydrophilic property, the 3D Ni-Zn anode achieved low Zn nucleation overpotential and induced the uniform Zn deposition without dendrite growth. However, some metal-based metals would result in a "top growth" mode, which can contribute to dendrite growth. To solve this problem, Shen *et al.*^[179] produced a stratified deposition framework (from bottom to top: Cu foam, Ni foam, and NiO) and realized stratified Zn deposition from bottom to top [Figure 6D]. It can be attributed to the different Zn deposition overpotentials and Zn affinity of metals. In addition to the dendrites, HER and other side reactions can also be suppressed via metal-based hosts. For instance, Jian *et al.*^[180] prepared a nanoporous Sn host (NSH) on a Cu mesh by the replacement reaction. With the high HER overpotential of Sn, NSH could suppress side reactions. Moreover, benefitting from the nanoporous structure, NSH also redistributed the Zn²⁺ flux and electric field to further uniform the Zn deposition. Nonetheless, due to their large weight, metal-based hosts may reduce the energy density to some extent.

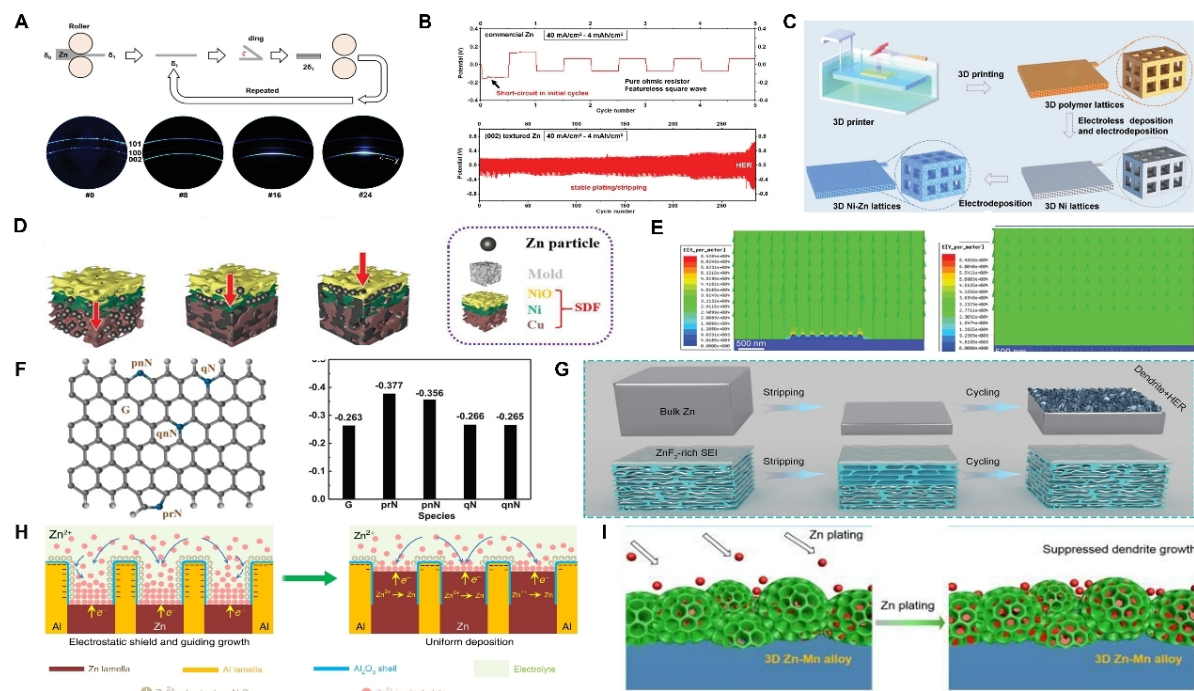


Figure 6. (A) Schematic diagram for ARB process and the 2D X-ray diffraction patterns of Zn foils before and after different ARB cycles ($2\theta = 36.2$ degrees). (B) The galvanostatic charge/discharge profile of commercial and textured Zn symmetric cells^[169]. (C) Schematic diagram of the fabrication process of 3D Ni-Zn anode^[178]. (D) Schematic illustrating stratified Zn deposition from bottom to top^[179]. (E) Electric field simulation on the Zn/CC anode surface before and after the deposition of CNT on CC^[182]. (F) Schematic illustration of graphene and different functional groups of N and corresponding binding energy with Zn atom^[188]. (G) Schematic illustration of Zn plating/stripping process on bulk Zn anode and MGA-Zn anode^[191]. (H) Schematic of morphology evolution for lamellar Zn₈₈Al₁₂ (at%) alloy anode^[31]. (I) Schematic illustration of the 3D Zn-Mn alloy for suppressed dendrite growth^[195]. Reproduced from Refs.^[169,178-179,182,188,191] and Refs.^[31,195] with permission from Wiley-VCH and Springer Nature.

Carbon-based 3D hosts have the advantage of light weight, which is conducive to improving the energy density of AZIBs. The excellent mechanical stability of carbon-based 3D hosts also gives them the ability to be used in flexible and wearable devices. Carbon fiber (CF) and carbon cloth (CC) purchased directly have poor hydrophilia and zincophilia^[181], which means that these carbon materials alone are insufficient to function as efficient hosts for Zn anodes. Many activated strategies have been developed within the 3D carbon frameworks to introduce Zn deposition sites and enhance the electrochemical performance of Zn anodes. For example, 3D CNT frames grown on CC using the CVD method enhanced the affinity with Zn and decreased the Zn nucleation overpotential^[182]. Moreover, the 3D CNT frames exhibited enlarged specific areas and a more uniform electric field distribution [Figure 6E]. Based on the merits, a higher CE of 97.9% and better cycle stability for 200 h at 2 mA cm^{-2} of anode were endowed. Other methods are also effective for stable Zn plating/stripping, such as depositing 3D CNT on CC^[182], printing Ag nanoparticles on CC^[183], and coating graphene on CF^[184]. Additionally, introducing defects^[185], zincophilic atoms^[186], or zincophilic functional groups^[187] are also efficient ways to activate the carbon matrix and strengthen interfacial interaction between Zn and the carbon matrix. For instance, Cao *et al.*^[188] introduced 3D nitrogen-doped vertical graphene nanosheets into the CC. They found that the binding energies of Zn²⁺ adsorbed on pyrrolic N (prN) (-0.377) and pyridinic N (pnN) (-0.356 eV) were larger than that of the carbon atomic group (-0.263 eV) [Figure 6F]. Therefore, the doped N could serve as nucleation sites for Zn²⁺ to reduce the Zn nucleation overpotential and lead to the homogeneous Zn deposition.

Apart from metal and carbon hosts, MXene is also a popular candidate for Zn host. It has been proven that $\text{Ti}_3\text{C}_2\text{T}_x$ MXene paper host can endow the Zn anodes with a suppressive dendrite growth and fast Zn plating/stripping kinetics because of its conductivity and hydrophilicity^[189]. Furthermore, an increased Zn deposition stability can be achieved when introducing zincophilic metals into the system^[190]. For instance, Tian *et al.*^[190] designed Sb nanoarrays on $\text{Ti}_3\text{C}_2\text{T}_x$ MXene paper. The Sb could function as a zincophilic nucleation seed to reduce nucleation overpotential and further regulate homogeneous Zn deposition. Nevertheless, 2D MXene paper is insufficient to accommodate large Zn deposition compared to the 3D structure. To address this issue, Zhou *et al.*^[191] constructed a 3D flexible MXene/graphene aerogel (MGA) scaffold, where the $\text{Ti}_3\text{C}_2\text{T}_x$ sheets were assembled onto the surface of rGO. Benefiting from the novel structure, MGA could effectively pack the deposited Zn. Moreover, the F terminal in the MXene could induce a ZnF_2 -rich SEI [Figure 6G], which was effective for uniform Zn deposition as well as inhibited byproduct ZHS formation and HER ($3.8 \times 10^{-3} \text{ mol h}^{-1} \text{ cm}^{-2}$)^[191]. In addition to MXene, some other novel hosts have also aroused research interest recently, such as MOF ZIF-8-500^[192] and TiOx/Zn/N-doped carbon inverse opal (TZNC IO) host^[193]. These novel frameworks are also efficient for a long lifetime of Zn anodes.

Zn alloy anodes

In addition to modulating the physical structure of Zn anodes, alloy design for Zn anodes is also a significant strategy through tuning the chemical constitution of Zn anodes^[194]. For instance, Wang *et al.*^[31] introduced an alternating lamellar $\text{Zn}_{88}\text{Al}_{12}$ (at%) alloy anode. They found that the Al layers could act as a 2D host to accommodate the deposited Zn, and the insulating Al_2O_3 shells generated on the Al layers could prevent the electrons transfer from Al to Zn^{2+} [Figure 6H]. These characters could guide Zn^{2+} deposition and finally achieve a dendrite-free behavior. Moreover, the alloy strategy can improve the stability of Zn anodes together with a 3D structure. Taking Zn-Mn alloy as an example, a Zn-Mn alloy with a 3D structure was obtained only using the electrodeposition method. The formed alloy anode could not only control the Zn^{2+} diffusion kinetics through favorable diffusion channels [Figure 6I] but also regulate Zn nucleation by a higher surface binding energy^[195]. As a result, the anode with a 3D Zn-Mn alloy could achieve 1900 stable cycles in the harsh conditions of 80 mA cm^{-2} and 16 mAh cm^{-2} in sea water-based aqueous electrolytes^[195].

To inhibit HER on Zn anodes, Wang *et al.*^[196] introduced Sn to alloy with Zn. The appropriate Sn amount could effectively suppress the HER due to the enlarged ΔG_{H}^* . Meanwhile, Sn could offer favorable sites to decrease the energy barrier for Zn nucleation, which would further regulate the Zn deposition and induce a dendrite-free behavior^[196]. In addition to Sn, Cu is a promising element to improve the corrosion resistance of alloy anodes. As is known, Cu possesses an intrinsically inert nature. The Cu-Zn alloy could effectively alleviate the HER and Zn corrosion^[197]. Moreover, the zincophilic Cu could also provide abundant Zn^{2+} adsorption sites to promote homogeneous Zn nucleation and deposition^[197]. Benefitting from the suppressed dendrites and side reactions, the Cu-Zn alloy anode achieved stable cycles for over 1600 h at 5 mA cm^{-2} and 2.5 mAh cm^{-2} in symmetric cells. It is worth noting that this Cu-Zn alloy anode could also enhance the electrochemical performance of cells in the alkaline system^[197].

MATERIAL DESIGNS OF ELECTROLYTES

The composition and concentration of electrolytes affect the anode–electrolyte interface, which is directly related to dendrites, HER, and the formation of byproducts. Zn salts used in AZIBs mainly include ZnSO_4 ^[198-201], $\text{Zn}(\text{CF}_3\text{SO}_3)_2$ ^[202-203], ZnCl_2 ^[204], $\text{Zn}(\text{BF}_4)_2$ ^[205], $\text{Zn}(\text{CH}_3\text{COO})_2$, $\text{Zn}(\text{NO}_3)_2$, $\text{Zn}(\text{ClO}_4)_2$ ^[206], and $\text{Zn}(\text{TFSI})_2$ ^[207]. Among them, ZnSO_4 is the most popular salt because of its stable property and low cost^[208]. Anions of Zn salts have important impacts on the electrolytes and anodes^[209-210]. For example, compared with SO_4^{2-} , the bulky CF_3SO_3^- can reduce the water amount around the Zn^{2+} to some extent and reshape the

Zn²⁺ coordination. Therefore, the Zn(CF₃SO₃)₂ electrolyte can reduce the solvation effect^[211] and even induce a preferred Zn (002) texture deposition^[212]. In addition to choosing suitable Zn salts, electrolyte regulation strategies, such as increasing electrolyte concentration, introducing electrolyte additives, employing hydrogel, and solid-state electrolytes, also have beneficial effects on the Zn anodes. Among them, hydrogel electrolytes can be obtained via introducing polymer directly or introducing monomer to induce polymerization in aqueous solutions containing Zn salts. Solid-state electrolytes can be prepared by dissolving Zn salts in a polymer network through non-aqueous solvent^[213] or hot-press casting^[214].

Highly concentrated electrolytes

Increasing the electrolyte concentration is a simple and effective strategy to improve the electrochemical performance of AZIBs. The merits of using concentrated electrolytes can be concluded in two ways. (1) Decreasing the amount of water molecules and breaking the hydrogen-bond networks in the bulk electrolyte: These are beneficial for reducing the side reactions, alleviating the active materials' dissolution, expanding the electrochemical stability window, and lowering the freezing point to some extent. (2) Changing the solvation structure of Zn²⁺^[215]: this can not only further govern the Zn deposition and suppress Zn dendrite growth, but it is also conducive to restrained side reactions. For instance, Zhang *et al.*^[216] found that the concentration of ZnCl₂ in aqueous could reach up to 30 m [where m is molality (mol kg⁻¹)], and the electrolyte would transform into a "water-in-salt" (WIS) electrolyte. Usually, with enough water molecules available, Zn²⁺ could be solvated to form stable [Zn(H₂O)₆]²⁺. However, the number of [Zn(H₂O)₆]²⁺ was minor in 30 m ZnCl₂ electrolyte because few free water molecules existed in this WIS^[216]. Moreover, there were fewer and fewer water molecules involved in the solvation structure of the Zn²⁺ with the increased ZnCl₂ concentration from 5 to 30 m. As a result, the concentration of [ZnCl₄]²⁻ would increase and that of [Zn(OH)₂Cl₄]²⁻ would decrease in the electrolyte. The average CE of the Zn anode could also increase from 73.2% to 95.4%^[216]. In addition to improving the reversibility of Zn plating/stripping, the 30 m ZnCl₂ WIS electrolyte also has the ability to mitigate the dissolution problem of active material^[217-218] and widen the voltage window^[218-219] compared to a dilute one.

Common electrolytes, such as ZnSO₄ and Zn(CF₃SO₃)₂ electrolytes, can also achieve improved electrochemical performance after increasing their concentration. For instance, 3 M [where M is molarity (mol L⁻¹)] ZnSO₄ electrolyte can not only suppress the dissolution of V₂O₅ cathode but also enhance the stability of the Zn anodes compared to that in 1 and 2 M electrolytes^[220]. Furthermore, with the ZnSO₄ concentration increasing from 2 to 4.5 M in the presence of 0.1 M MnSO₄ electrolyte additives, strongly aggregated ion pairs would replace the water molecules around Zn²⁺^[199]. Therefore, the concentrated electrolyte of 4.2 M ZnSO₄ + 0.1 M MnSO₄ obtained an improved Zn plating/stripping CE of 99.21%^[199]. A similar phenomenon is evidenced in the Zn(CF₃SO₃)₂ electrolyte, where the CE of full batteries in Zn(CF₃SO₃)₂ electrolyte increases with salt concentration boosting from 1 to 4 M^[208]. However, the saturation concentration of most Zn salts is limited at ~4 M^[221-222] or even smaller^[206], where a lot of free water exists and most Zn²⁺ ions are surrounded by six water molecules. In view of this, researchers attempted to add other salts in Zn electrolytes to obtain highly concentrated electrolytes. These highly concentrated electrolytes can also decrease the water molecules and alter the solvation structure of Zn²⁺^[223-224]. For instance, a saturated WIS electrolyte was investigated by introducing 20 m LiTFSI into 1 m Zn(TFSI)₂^[225]. In this novel WIS electrolyte, water molecules could be severely confined within the Li⁺ solvation structures, and the Zn²⁺-solvation sheath was occupied primarily by TFSI⁻ to form (Zn-TFSI)⁺ structure^[225]. The changed Zn²⁺-solvation sheath could improve the reversibility of the Zn anodes (CE ~ 100%) and simultaneously restrain the side reactions. However, it is worth noting that Zhang *et al.*^[226] recently found that Zn²⁺ was still mainly solvated by six waters in the first solvation shell in 1 m Zn(TFSI)₂ + 20 m LiTFSI electrolyte. Therefore, more studies need to be developed in this electrolyte system. In addition to the changed Zn²⁺ solvation structure, researchers found that an enhanced threshold of critical current density

for cation depletion could also result in regulated Zn deposition and suppressed dendrite growth in the highly concentrated electrolyte^[227].

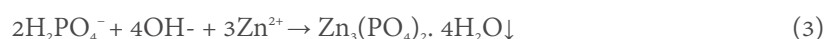
Electrolyte additives

In addition to the concentration control, the composition change of an electrolyte via a small amount of electrolyte additives can also affect the stability of Zn anodes. Electrolyte additives can be mainly divided into inorganic and organic additives.

Inorganic additives

Some metal ions have more negative reduction potential than Zn²⁺, such as Mn²⁺^[199], Na⁺^[228], Li⁺^[229], *etc.* As a result, these metal ions can competitively adsorb on the Zn protrusions and thus inhibit the dendrite growth according to an electrostatic shield mechanism. For instance, Li⁺ can adsorb on the Zn anode surface and further establish a new interface between the anode and electrolyte. The new interface can guide non-dendrite Zn growth and inhibit the HER^[230]. Additionally, the Li₂O/Li₂CO₃ layer could be preferentially formed on the Zn surface to provide a shielding effect when adding 2 M LiCl into 3 M ZnSO₄^[229]. It is worth noting that, in addition to metal ions, other inorganic cations (such as NH₄⁺^[231-233]) can also adsorb on the Zn protrusions and regulate the Zn deposition process. Furthermore, some metal ions can inhibit the Zn dendrite growth by regulating the Zn nucleation process. For instance, Li *et al.*^[234] found that Ce³⁺ and La³⁺ could guide the Zn nucleation through a progressive process instead of an instantaneous one, thereby resulting in stable Zn stripping/plating behavior.

In addition to guiding Zn deposition directly, the introduced inorganic salts can also in situ form an SEI protective layer on the Zn surface to stabilize the anode-electrolyte interface^[235]. In LIBs, SEI layers can be in situ built at the anode surface through the decomposition of electrolyte components and/or salt anions^[236]. However, in AZIBs, SEI with in situ formation remains a huge challenge. It can be attributed to that the relatively high reduction potential of Zn deposition and restricted voltage windows of water. As a result, HER and Zn plating are usually generated prior to the decomposition of salt anions. To in situ form SEI on Zn anodes, several mechanisms or methods have been developed by adding inorganic salts. One of these is to make use of the locally increased OH⁻ caused by HER. For instance, Zeng *et al.*^[237] found that a dense and uniform Zn₃(PO₄)₂·4H₂O SEI could form by adding Zn(H₂PO₄)₂ to Zn(CF₃SO₃)₂ electrolyte. As shown in Figure 7A, through the chemical reaction



the Zn₃(PO₄)₂·4H₂O film would precipitate on the anode as SEI with the increased OH⁻ leftover from HER. Similarly, ZnF₂-Zn₅(CO₃)₂(OH)₆-organic bi-layer SEI was produced by introducing Zn(NO₃)₂ additive into Zn(CF₃SO₃)₂ aqueous electrolyte^[238]. This bi-layer SEI could promote Zn²⁺ diffusion and block water penetration, thus enabling a highly reversible Zn plating/stripping (CE ~ 99.8%)^[238]. In addition to utilizing the increased OH⁻, another method is to add salts that are thermodynamically instable in aqueous environments. Inspired by this, Chu *et al.*^[239] added KPF₆ in 2 M ZnSO₄ aqueous electrolyte. They found that a composite SEI (ZCS) could be in situ formed on the Zn anode, and the ZCS was mainly composed of Zn₃(PO₄)₂ and ZnF₂. It could be attributed to the decomposition of PF₆⁻ and the further reaction between the decomposition products and Zn. Benefitting from the in situ formed ZCS, the largest cumulative capacity on the anode could reach up to 2020 mAh cm⁻² and the symmetric cells realized stable cycles for 250 h at 10 mA cm⁻² and 20 mAh cm⁻². In addition to the above two methods, SEI can also be formed in Zn anodes when introducing some metal ions with higher reduction potential than Zn²⁺, such as Bi³⁺, Pd²⁺^[240], Sn²⁺^[241-242], In³⁺^[243], *etc.* These metals could preferentially deposit on the anodes before Zn and thus can act as SEI

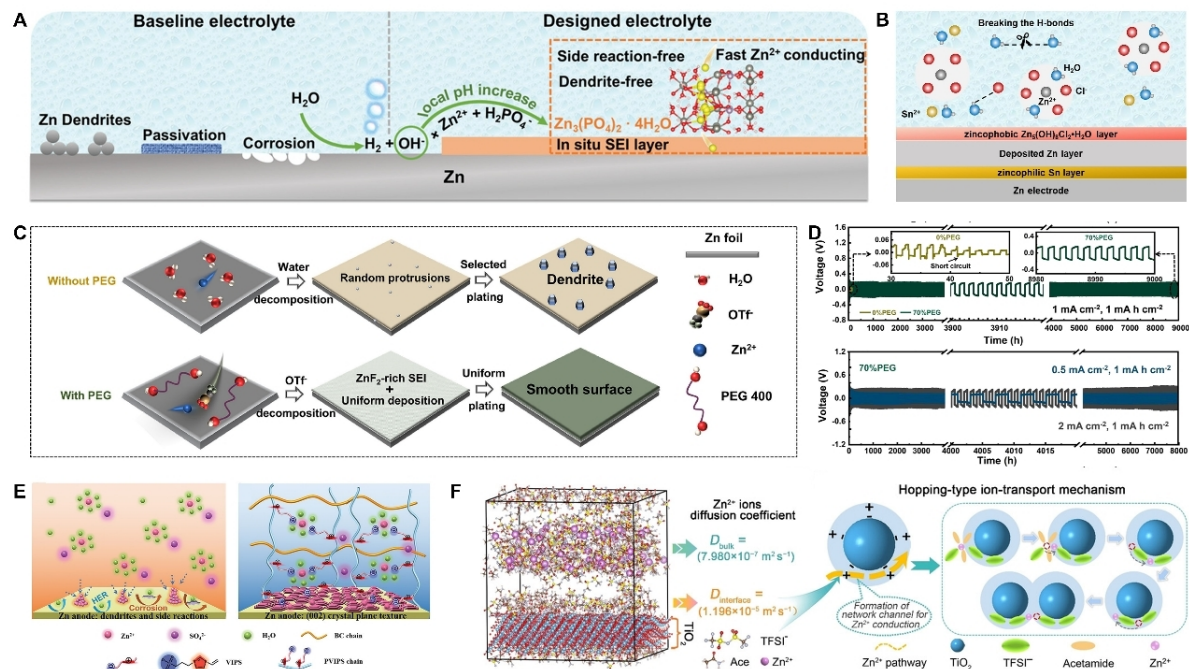


Figure 7. (A) Schematic diagram of the in situ formation of $Zn_3(PO_4)_2 \cdot 4H_2O$ SEI on Zn anode surface^[237]. (B) Schematic diagram of preferential Sn deposition than Zn in the 7.6 m $ZnCl_2$ aqueous electrolyte with 0.05 m $SnCl_2$ additive. The deposited Sn would further facilitate the formation of a uniform zincophobic $Zn_5(OH)_3Cl_2 \cdot H_2O$ SEI, and the water activity was decreased due to the strong H_2O-Cl^- interactions^[241]. (C) Schematic illustration of the PEG additive in the electrolyte for uniform Zn deposition. (D) The galvanostatic charge/discharge profile of symmetric cells with 0% or 70% PEG additive^[284]. (E) Schematic diagram of PVIPS gel electrolyte for changing the solvated structure of Zn^{2+} and inducing a Zn (002) texture^[311]. (F) The MD simulation snapshot of ZCE at 300 K illustrating the enhanced ion dynamics and the diagram illustrating the Zn^{2+} hopping-type transport mechanism in the ZCE^[329]. Reproduced from Refs. ^[237,241,311,329], and Ref. ^[284] with permission from Wiley-VCH and Elsevier.

layers to guide Zn deposition and suppress the side reactions [Figure 7B].

Organic additives

The other popular and effective candidate of electrolyte additives are organic additives, including alcohols^[244-247], ether^[248-252], aldehydes^[253-254], esters^[255-256], amino acid^[257], polymers^[258-259], organic salts^[259-266], etc. The organic additives usually function as trace mineral supplements or co-solvent. They can affect Zn deposition in three ways.

Firstly, they prefer to adsorb on the surface or protuberance of the Zn anodes due to their stronger absorptive function than H_2O ^[254] or because of the tip effect^[267]. The adsorbed organic additives can not only occupy the active sites for HER and further alleviate side reactions^[263] but also serve as zincophilic sites for Zn nucleation and restricting 2D Zn^{2+} diffusion^[268]. As a result, these organic additives can suppress the continuous dendrite growth and even guide different crystallographic orientations and surface textures of deposited Zn^[269]. Secondly, organic additives can inhibit the invasion of free water into the Helmholtz plane^[270] or change the Zn^{2+} solvation structure^[271-272]. The changed solvation structure would guide Zn deposition and even interrupt the hydrogen bonding network among water molecules^[273] to reduce water activity. The reduced water activity can not only broaden the electrochemical stability window^[274] but also lower the freezing point of the electrolyte^[275]. These are beneficial to the inhibited side reactions and the further expanded usage of AZIBs. More importantly, an SEI could be in situ formed, driven by the decomposition of organic additives^[276] or polymerization. For instance, Zeng *et al.*^[277] found that a stable

polydopamine SEI could be constructed via an in situ electrochemical polymerization of dopamine additive. In addition to the polymerization, the introduced organic additives can be decomposed on the anodes to form SEI layers due to the inhibited HER after excluding water in the EDL structure^[278]. Benefitting from the three effects on the anodes, some organics have been frequently studied as additives in AZIBs, such as DMSO^[279-280] and PEG^[281-283]. Wu and co-workers^[284] found that the PEG additive had several advantages at the same time. These advantages included enabling Zn (002) deposition preferentially, decreasing the water activity, and forming an anion-dominated solvent structure and ZnF₂-rich SEI films [Figure 7C]. Benefitting from these merits, the Zn anode in electrolyte with 70% PEG additive achieved a super-high cyclic performance for 9000 or 8000 h at 1 or 2 mA cm⁻² [Figure 7D]^[284].

Hydrogel and solid-state electrolytes

Employing the hydrogel/quasi-solid electrolytes is also considered a promising solution to Zn anode issues because of their limited water content and decent ionic conductivity. They are generally composed of Zn salts and polymer skeleton networks, including non-crosslinked and crosslinked hydrogel electrolytes^[285]. Unlike the crosslinked type, non-crosslinked hydrogel electrolytes tend to exhibit amorphous morphology and poor mechanical properties; thus, they require additional separators in most cases. Based on different polymer skeletons, the hydrogel electrolytes used in AZIBs can mainly be divided into PEO-based^[286], PVDF-based^[287], PAN-based^[288], PVA-based^[289-293], PAM-based^[294-299], natural biomass-based^[300-304], *etc.* Appropriate Zn salts should be selected to match the polymers because some polymers are incompatible with salts. For example, commonly used polymers (PEO, PVA, agar, gelatin, and sodium polyacrylate) in AZIBs would precipitate in electrolytes containing SO₄²⁻ according to the Hofmeister series^[305]. Similar to polymer electrolyte additives, polymer chains of hydrogel electrolytes can closely adsorb onto the Zn anodes, especially on the bulge. These polymer chains can serve as electrostatic shielding layers to inhibit dendrite growth and prevent water from contacting the anodes^[306]. Moreover, polymers can guide Zn²⁺ transport and deposition through local segmental motion because the Zn²⁺ would coordinate with oxygen-containing functional groups on the polymer chains^[302,307-310]. For instance, Hao *et al.*^[311] found that, in polyzwitterionic PVIPS gel electrolyte, the SO₃⁻ groups could bond to Zn²⁺ and change the Zn²⁺ solvation structure from [Zn(H₂O)₆]²⁺ to R-SO₃⁻[Zn(H₂O)₄]²⁺-SO₃⁻R [Figure 7E]. The changed solvated Zn²⁺ would further guide the Zn²⁺ transport and inhibit the side reactions. Moreover, the imidazole groups in PVIPS gel electrolyte were able to synergize with SO₃⁻ groups to guide Zn²⁺ nucleation and deposition along the (002) plane. Most crosslinked hydrogel electrolytes exhibit high mechanical integrity, which is beneficial to suppress dendrite formation^[312]. However, the hydrogel electrolytes with high modulus may cause poor interfacial contact with anodes. To solve this, Cao *et al.*^[313] developed a mechanoadaptive morphing gel electrolyte (MorphGE). MorphGE with high modulus effectively inhibited Zn dendrite growth under the well interfacial contact with Zn anodes. Moreover, MorphGE also relieved the side reactions due to its anchoring for desolvated Zn²⁺. As a result, MorphGE induced long cycles for 2400 h at 1 mA cm⁻² and 1 mAh cm⁻², and even 100 h at 10 mA cm⁻² and 10 mAh cm⁻² in symmetrical Zn cells. It is worth noting that the hydrogel electrolytes can expand the application of AZIBs in flexible and wearable energy storage devices^[314].

All-solid-state electrolytes can fundamentally eliminate the side reactions driven by water, thus improving the utilization of Zn anodes. However, few studies on all-solid electrolytes have been reported^[315]. That is because the divalent Zn²⁺ has a higher charge density, which induces quite sluggish diffusion kinetics in solid materials at room temperature^[316]. Water can activate inorganic electrolytes to some extent. For example, MOF-based Zn²⁺ solid electrolytes^[317] and inorganic colloidal electrolytes^[318-319] have been explored to obtain good Zn²⁺ migration and suppression ability for both dendrites and side reactions. However, their Zn²⁺ conduction mechanism is actually Zn²⁺ being transported through water. Recently, an inorganic Zn²⁺ conductor electrolyte (ZHAP-Zn) with a solid-liquid hybrid Zn²⁺ transport channel has been developed^[320].

The ZHAP-Zn enabled a high Zn^{2+} transference number of 0.75 and achieved dendrite-free Zn plating/stripping over 2000 h at 0.5 mA cm^{-2} . Nevertheless, the use of all-solid-state electrolytes without water can still be a challenge. In general, polymers with lower glass transition temperatures^[321] and all-amorphous regime^[322] present higher ionic conductivity and can be used in AZIBs. Additionally, the use of inorganic fillers (such as TiO_2 ^[323-324], ZrO_2 ^[321], Al_2O_3 ^[325], MXene^[326], *etc.*) and the bulky anionic salts^[327-328] can effectively reduce the crystallinity of the polymer to improve Zn^{2+} conductivity, but their influence on Zn dendrites is rarely researched. Very recently, a Zn^{2+} conductive solid electrolyte (ZCE) was prepared and studied for the Zn anode by crystallization of $\text{Zn}(\text{TFSI})_2$ -based deep eutectic solvent^[329]. In ZCEs, TFSI^- was preferentially adsorbed on the surface of Lewis acid TiO_2 , thus weakening ion association and resulting in a high Zn^{2+} transference number (0.64). Moreover, an interface Zn^{2+} conduction pathway was established via the adsorbed TFSI^- on the surface [Figure 7F], which endowed ZCEs with a high ionic conductivity of $5.91 \times 10^{-5} \text{ S cm}^{-1}$ at $30 \text{ }^\circ\text{C}$. Benefitting from the good Zn^{2+} conductivity, sufficient mechanical strength, and water-free characteristics, the ZCEs induced Zn plating/stripping for 4000 h at 0.01 mA cm^{-2} without dendrites or side reactions. However, the ionic conductivity of all-solid-state electrolytes is still far below the practical application requirements, and the research for all-solid-state Zn-ion batteries is still in the initial stages.

CONCLUSIONS AND OUTLOOK

AZIBs have attracted extensive attention because of their advantages of low price, high safety, and high power density. However, the anode-electrolyte interface is often accompanied by some harmful problems that hinder the performance of AZIBs. Due to the uneven distribution of electric field and Zn^{2+} concentration field, dendrite growth often exists on the Zn anodes, causing the battery to short circuit. In addition to Zn dendrites, another big issue on Zn anodes is the side reactions (HER, corrosion, and passivation) driven by the thermodynamic activity of Zn metal in an aqueous solution. The side reactions could reduce Zn utilization and the CE of the Zn plating/stripping on Zn anodes. For this, material designs for the anodes and electrolytes have been developed. For instance, on the Zn anodes, protective layers can physically isolate the anodes and bulky electrolytes, thus alleviating the side reactions. Moreover, layers of modified Zn anodes or separators can also regulate Zn^{2+} transfer kinetics deposition and induce a dendrite-free deposition behavior. In the electrolyte, trace amounts of electrolyte additives can regulate the solvated structure of Zn^{2+} to guide uniform Zn deposition and mitigated side reactions. More detailed information about material designs for stable Zn anodes can be seen in Table 1. Although the material design for Zn protection has made many advances, there are still some factors limiting their actual application from the lab to commercialization, and further research efforts are needed.

(1) Surface modification of Zn is recognized as an effective strategy to stabilize Zn metal anodes. At present, numerous inorganic and organic materials have been explored for modifying the Zn anode surface. Zn anodes modified by these materials achieve enhanced electrochemical performance. However, most buffer coatings are made using the doctor-blading method and thus suffer from poor bonding strength. They are prone to peel off due to the repeated volume changes during cycles. Therefore, more methods need to be developed to enhance the contact between the layers and anodes during cycling. For instance, the protective layers realized via in situ formation have a tight bond with Zn. However, the rigid and fragile nature of in situ Zn^{2+} -conducting materials or organic layers with low ion conductivity may induce limited area capacity and DOD of the Zn anodes. Composite coatings inherit the advantages of several materials and thus can achieve synergistic effects to greatly improve the stability of Zn anodes. Therefore, in situ constructing composite layers with high flexibility and Zn^{2+} conductivity on the Zn anodes is a strategy worth considering in the future.

Table 1. Summary of different material design strategies for stable Zn anodes

Designs	Materials	Synthesis	Important parameter (electrolyte or salt)	Representative indicators			Reference	Remarks ^b			
				Symmetric cells	Asymmetrical cells						
					Lifespan (h) (C _r , C ₂) ^a	CE			Cycles (C _r , C ₂) ^a		
Surface modification on Zn metal	Carbon-based materials	CG separator	Casting	2 M ZnSO ₄	1750 (2, 1) 400 (20, 10)	98.68%	100 (1, 1)	[50]	<ul style="list-style-type: none"> •Simple preparation •Redistribution of surface electric •Less effect on large DOD 		
		HsGDY	In situ growth	2 M ZnSO ₄	2400 (0.5/1/2, 0.1)	/	/	[55]			
		N-C	Casting	2 M ZnSO ₄	1000 (1, 1)	98.76%	120 (2, 2)	[42]			
		CNG	Drying	3 M ZnSO ₄	2956 (1, 0.5)	99.4%	300 (/ , 0.5)	[46]			
	Inorganic compounds	ZrO ₂	Casting	2 M ZnSO ₄	3800 (0.25, 0.125) 2100 (5, 1)	99.36%	230 (20, 5)	[57]	<ul style="list-style-type: none"> •Simple preparation •Physical barrier for free water •Crack on the large DOD 		
		ZnO	Liquid-phase synthesis	2 M ZnSO ₄ + 0.1 M MnSO ₄	500 (5, 1.25)	99.55%	300 (2, 0.5)	[63]			
		ZnS	CVD	1 M ZnSO ₄	1100 (2, 2)	99.2%	200 (2, 1)	[68]			
		ZnF ₂	In situ ion metathesis	2 M ZnSO ₄	2500 (1/2/5, 1)	-99.5%	1000 (1, 1)	[73]			
		MXene	In situ reducing/assembling	2 M ZnSO ₄	800 (0.2, 0.2)	/	/	[90]			
		ZnP	Electrodeposition	2 M ZnSO ₄	3200 (5, 1.25) 300 (20, 30)	99.5%	200 (2, 0.5)	[77]			
		CaCO ₃	Casting	3 M ZnSO ₄ + 0.1 M MnSO ₄	836 (0.25, 0.05)	/	/	[83]			
		BaTiO ₃	Coating		4000 (1, 1) 1300 (10, 2)	/	120 (1, 1)	[85]			
		Organic compounds	PA	Casting	2 M ZnSO ₄	8000 (0.5, 0.25)	95.12%	300 (0.4, 0.4)		[102]	<ul style="list-style-type: none"> •Simple preparation •Physical barrier for free water •Certain shape adaptability •Lower ionic conductivity
			FCOF	Pulling	2 M ZnSO ₄	1700 (5, 1)	97.2%	320 (80, 1)		[110]	
	Gelatin		Casting and crosslinking	1 M Zn(OTF) ₂	4000 (1, 1)	/	/	[114]			
	MOF		Casting	2 M ZnSO ₄	3000 (0.5, 0.5)	/	/	[116]			
	Metal-based materials		ZnSe	CVD	2 M ZnSO ₄	1500 (1/10, 1)	/	/	[128]	<ul style="list-style-type: none"> •Simple preparation •Redistribution of surface electric •Certain solutions for side reactions •Less effect on large DOD 	
		In	Ion exchange	2 M ZnSO ₄	1400 (0.25, 0.05)	/	/	[136]			
		Cu/Zn	Ion exchange and annealing	3 M ZnSO ₄	1500 (1, 0.5)	91.8%	100 (5, 0.5)	[33]			
Ga-In		Coating	3 M ZnSO ₄	2100 (0.25, /)	/	/	[141]				

					0.05) 1200 (1, 0.1)				
The structure and constitution design of Zn anodes	Multimaterial composites	AEC (TiO ₂ -PVDF)	Coating	2 M ZnSO ₄	2000 (0.885, 0.885)	99.4%	1000 (1.77, 0.885)	[153]	•Simple preparation •Physical barrier for free water
		Nafion Zn-X	Casting	2 M ZnSO ₄	2000 (5, 0.5)	97%	130 (0.5, 0.5)	[150]	•More complicated mechanism •At initial stage
	Zn surface structure designs	Ti ₃ C ₂ T _x MXene/ZnS	Coating	2 M ZnSO ₄	1100 (1, 0.5/1) 400 (5, 5)	/	/	[159]	
		Pitted surface texture	Etching	2 M ZnSO ₄	1000 (1, 1)	/	/	[164]	•Redistribution of surface electric
		hexagonal-hole patterns	Etching	2 M ZnSO ₄	1800 (0.5, 0.5)	99.57%	700 (2, 1)	[165]	•Poor solution for side reactions
		3D porous surface	Etching	1 M ZnSO ₄	930 (4, 2)	/	/	[166]	
	Conductive host designs	PPZ@Zn	Etching	2 M ZnSO ₄	3000 (1, 0.5)	/	/	[167]	
		SDF	Template, deposition and sputtering	2 M ZnSO ₄	1000 (2, 1)	/	/	[179]	•Redistribution of surface electric and ion flux
		MGA	Freeze-drying	2 M ZnSO ₄	1050 (10, 1)	99.67%	600 (10, 1)	[191]	•Beneficial to more Zn and large DOD
		3D Ti-TiO ₂	Electrodeposition and dealloying	2 M ZnSO ₄	2000 (1, 1)	95.20%	200 (10, 5)	[177]	•Lower volume energy density •Poor solution for side reactions
Zn alloy anodes	Zn ₈₈ Al ₁₂ (at%)	Metallurgy	2 M ZnSO ₄ without O ₂	2000 (0.5, /)	100% ^c	/	[31]	•Dendrite-free	
	Zn ₃ Mn	Electrodeposition	2 M ZnSO ₄ in seawater	760 (80, 16)	100% ^c 99.62%	/ 2500 (10, /)	[195]	•Certain solutions for side reactions •Less effect on large DOD	
Design of electrolytes	Highly concentrated electrolytes	30 m ZnCl ₂	/	/	600 (0.2, -0.033)	95.4% ^d	/	[216]	•Simple preparation •Potential for large DOD
		3 m Zn(Otf) ₂ +17 m NaClO ₄	/	/	1600 (1, 0.25)	-99.96%	700 (0.5, 0.25)	[224]	•Higher cost •Higher viscosity
		1 m Zn(TFSI) ₂ + 20 m LiTFSI	/	/	170 (0.2, -0.033)	-100% ^c	/	[225]	•Lower ionic conductivity
	Electrolyte additives	50 mM NH ₄ Oac	/	2 M ZnSO ₄	3500 (1, 1)	99.7%	1800 (1, 0.5)	[233]	•Simple preparation •Low cost
		25 mM Zn(H ₂ PO ₄) ₂	/	1 M Zn(OTF) ₂	1200 (1, 1)	99.4%	400 (/ , 0.5)	[237]	•Potential for large DOD •More complicated mechanism
		0.05 M KPF ₆	/	2 M ZnSO ₄	1200 (2, 4)	99.37%	90 (4, 2)	[239]	
		300 mM In(Otf) ₃	/	3 M Zn(OTF) ₂	5700 (2, 2)	99.94%	1931 (0.5, 0.5)	[243]	
		70 wt% PEG	/	1M Zn(OTF) ₂	9000 (1, 1) 8000 (0.5/2, 1)	/	/	[284]	
0.5 m Me ₃ EtNOTF	/	4 m Zn(OTF) ₂	6000 (0.5,	99.8%	1000 (0.5,	[276]			

	DMSO	H ₂ O/DMSO = 4.3:1 (vol.%)	1.3 m ZnCl ₂	0.25)	1000 (0.5, 0.5)	99.5%	400 (1, 0.5)	[280]	
Hydrogel and solid-state electrolytes	PVIPS	Crosslinking	ZnSO ₄	500 (5, 5)	500 (5, 5)	99.6%	400 (1, 1)	[311]	•Certain mechanical strength
	PVA-B-G	Crosslinking	ZnSO ₄ + MnSO ₄	1400 (2, 2)	/	/	/	[292]	•Multifunctional, such as flexible, self-healing, freeze-tolerant
	polyzwitterionic PSBMA	Crosslinking	ZnSO ₄	3500 h (0.5, 0.5)	/	/	/	[303]	•Reduced amount of free water
	ZS/GL/AN	Thermal initiation method	ZnSO ₄	3000 (0.2, 0.2)	3000 (0.5, 5)	/	/	[307]	•Intolerance for some Zn salt
	PAMPSZn	Ion exchange and crosslinking	/	4500 (1, 1)	4500 (1, 1)	99.3%	400 (/ , /)	[309]	•Low ionic conductivity
	ZHAP-Zn	Ion exchange and pressing	/	2000 (0.5, 0.125)	2000 (0.5, 0.125)	/	/	[320]	•Low power density
	ZCE	Crystallizing solvent	Zn(TFSI) ₂	4000 (0.01, 0.005)	4000 (0.01, 0.005)	/	/	[329]	•Aging problem

^a(C₁, C₂), current density (mA cm⁻²) and area capacity (mAh cm⁻²); ^bother features besides dendrite-free; ^cthe CE is obtained through chronocoulometric curves; ^dthe CE measurement is followed by a “reservoir” galvanostatic protocol established by Zhang’s group^[330-331] and Ma et al.^[332-333], the CE using a “reservoir free” galvanostatic protocol unless otherwise specified.

(2) The structure and constitution designs of Zn anodes are significant for stable Zn anodes. The change in surface morphology of Zn metal can effectively regulate Zn deposition and alleviate dendrite growth. However, as the deposited Zn increases, the effect of the original surface morphology becomes smaller, and Zn dendrites may still grow. Compared with typical 2D Zn anodes, 3D anodes can not only accommodate more deposited Zn and larger volume variation, but also effectively reduce the local current density and redistribute the electric field due to its high specific surface area and good electrical conductivity. Nevertheless, the 3D skeleton cannot prevent side reactions, and, conversely, the nanoscale host may accelerate the reaction kinetics of side reactions due to its more active sites. The alloy strategy can inhibit HER by introducing elements with inert nature or higher HER overpotential. The formed alloy can guide the Zn deposition to some extent but may also fail when the alloy surface is completely covered by the deposited Zn. Cooperative strategies combining structure design with alloy strategy, surface protection, or hydrogel electrolyte may be workable plans for a higher electrochemical performance of Zn anodes.

(3) Modulating the composition and concentration of electrolytes is a promising way to optimize the anode-electrolyte interface and promote the utilization of Zn anodes. Introducing electrolyte additives is considered an effective method to reduce Zn dendrites. In addition to protecting the anodes, they can also act on the cathode and thus affect the whole battery. For example, organic additives usually lead to increased polarization that further deteriorates the rate performance of AZIBs, and the inorganic ones may complicate the battery system. Therefore, an in-depth study of additives for anodes and cathodes should be considered. Moreover, exploring composite additives is a possible way to obtain a better performance of AZIBs. High concentration electrolytes, especially “water-in-salt” electrolytes, can change the Zn²⁺ solvation structure, thus restraining the dendrite growth and side reactions. However, the concentrated electrolytes usually cause high cost, high viscosity, and decreased ionic conductivity. Balancing the trade-offs of various aspects, such as enhancing the Zn

utilization, keeping high Zn^{2+} conductivity, and maintaining a low cost, is highly demanded. Hydrogel or solid-state electrolytes can also solve the Zn anode issues due to their less water amount and suitable mechanical strength. Their extra mechanical properties also expand the application of AZIBs to the flexible and wearable fields. However, their poor contact with anodes and low intrinsic ion conductivity are major headaches for their further development. Although some inorganic fillers are conducive to enhancing ionic conductivity of hydrogel or solid-state electrolytes, corresponding studies are rare and their effects on Zn anodes are still not clear. To improve the power density of AZIBs, the development of hydrogel or solid-state electrolytes with high ionic conductivity and high dynamic adaptability is still urgently needed.

(4) Although the material design strategies of Zn anodes have been investigated and developed, the in-depth understanding of these issues and strategies to improve the performance of the Zn anodes are limited and still in the lab. There are still many problems to be solved for achieving the practical application of AZIBs. For instance, the test protocols of Zn anodes are not unified. It means that the different studies and strategies lack comparability to a certain extent. In addition, current material design strategies of Zn anodes are mostly based on excess Zn and small DOD, which may fall short of commercial requirements and cover up the shortcomings of strategies. Moreover, the compatibility of material designs for stabilizing Zn anodes with cathode materials needs more exploration, especially the designs on electrolytes. Besides, the basic advantages of AZIBs, such as low cost and high safety, cannot be thrown away during the development. Therefore, it is recommended that a test standard that meets commercial requirements, including the current density and DOD, should be urgently formulated to accelerate the practical application of AZIBs. The cost and safety should also be evaluated simultaneously for the further large-scale development of AZIBs.

DECLARATIONS

Authors' contributions

Selecting the topic and conceiving the structure of this paper: Zhou WY, Niu ZQ
Investigation, formal analysis, writing-original draft: Zhang YJ
Writing-review & editing: Bi SS, Niu ZQ, Zhou WY, Zhang YJ
Funding acquisition, supervision: Zhou WY, Xie SS

Availability of data and materials

Not applicable.

Financial support and sponsorship

This work was supported by the National Key Research and Development Program of China (Grant No. 2018YFA0208402; No. 2019YFA0705600; No. 2020YFA0714700), the National Natural Science Foundation of China (Grant No. 11634014; No. 52172060; No. 51372269), and the Strategic Priority Research Program of Chinese Academy of Sciences (Grant No. XDA09040202).

Conflicts of interest

All authors declared that there are no conflicts of interest.

Ethical approval and consent to participate

Not applicable.

Consent for publication

Not applicable.

Copyright

© The Author(s) 2021.

REFERENCES

1. Li Y, Fu J, Zhong C, et al. Recent advances in flexible zinc-based rechargeable batteries. *Adv Energy Mater* 2019;9:1802605. DOI PubMed
2. Yu P, Zeng Y, Zhang H, Yu M, Tong Y, Lu X. Flexible zn-ion batteries: recent progresses and challenges. *Small* 2019;15:e1804760. DOI PubMed
3. Gao X, Zhang H, Liu X, Lu X. Flexible Zn-ion batteries based on manganese oxides: Progress and prospect. *Carbon Energy* 2020;2:387-407. DOI
4. Zhao S, Zuo Y, Liu T, et al. Multi-functional hydrogels for flexible zinc-based batteries working under extreme conditions. *Adv Energy Mater* 2021;11:2101749. DOI
5. Kong L, Tang C, Peng H, Huang J, Zhang Q. Advanced energy materials for flexible batteries in energy storage: A review. *SmartMat* 2020;1:smm2.1007. DOI
6. Wu M, Zhang G, Yang H, et al. Aqueous Zn-based rechargeable batteries: recent progress and future perspectives. *InfoMat*. DOI
7. Ma Y, Ma Y, Diemant T, et al. Unveiling the intricate intercalation mechanism in manganese sesquioxide as positive electrode in aqueous Zn-metal battery. *Adv Energy Mater* 2021;11:2100962. DOI
8. Zhang N, Cheng F, Liu J, et al. Rechargeable aqueous zinc-manganese dioxide batteries with high energy and power densities. *Nat Commun* 2017;8:405. DOI PubMed PMC
9. Huang J, Wang Z, Hou M, et al. Polyaniline-intercalated manganese dioxide nanolayers as a high-performance cathode material for an aqueous zinc-ion battery. *Nat Commun* 2018;9:2906. DOI PubMed PMC
10. Chao D, Zhou W, Ye C, et al. An electrolytic Zn-MnO₂ battery for high-voltage and scalable energy storage. *Angew Chem Int Ed Engl* 2019;58:7823-8. DOI PubMed
11. Wan F, Niu Z. Design strategies for vanadium-based aqueous Zinc-ion batteries. *Angew Chem Int Ed Engl* 2019;58:16358-67. DOI PubMed
12. Wan F, Huang S, Cao H, Niu Z. Freestanding potassium vanadate/carbon nanotube films for ultralong-life aqueous Zinc-Ion batteries. *ACS Nano* 2020;14:6752-60. DOI PubMed
13. Konarov A, Voronina N, Jo JH, Bakenov Z, Sun Y, Myung S. Present and future perspective on electrode materials for rechargeable Zinc-Ion batteries. *ACS Energy Lett* 2018;3:2620-40. DOI
14. Ma L, Chen S, Li H, et al. Initiating a mild aqueous electrolyte Co₃O₄/Zn battery with 2.2 V-high voltage and 5000-cycle lifespan by a Co(iii) rich-electrode. *Energy Environ Sci* 2018;11:2521-30. DOI
15. Zhao Y, Wang D, Li X, et al. Initiating a reversible aqueous Zn/Sulfur battery through a “liquid film”. *Adv Mater* 2020;32:e2003070. DOI PubMed
16. Song J, Xu K, Liu N, Reed D, Li X. Crossroads in the renaissance of rechargeable aqueous zinc batteries. *Materials Today* 2021;45:191-212. DOI
17. Wang X, Wang F, Wang L, et al. An aqueous rechargeable Zn//Co₃O₄ battery with high energy density and good cycling behavior. *Adv Mater* 2016;28:4904-11. DOI PubMed
18. Yuan X, Wu X, Zeng X, et al. A fully aqueous hybrid electrolyte rechargeable battery with high voltage and high energy density. *Adv Energy Mater* 2020;10:2001583. DOI
19. Zampardi G, La Mantia F. Open challenges and good experimental practices in the research field of aqueous Zn-ion batteries. *Nat Commun* 2022;13:687. DOI PubMed PMC
20. Yuan X, Ma F, Zuo L, et al. Latest advances in high-voltage and high-energy-density aqueous rechargeable batteries. *Electrochem Energy Rev* 2021;4:1-34. DOI
21. Wu K, Huang J, Yi J, et al. Recent advances in polymer electrolytes for Zinc ion batteries: mechanisms, properties, and perspectives. *Adv Energy Mater* 2020;10:1903977. DOI
22. Zhang T, Tang Y, Guo S, et al. Fundamentals and perspectives in developing zinc-ion battery electrolytes: a comprehensive review. *Energy Environ Sci* 2020;13:4625-65. DOI
23. Yuan L, Hao J, Kao C, et al. Regulation methods for the Zn/electrolyte interphase and the effectiveness evaluation in aqueous Zn-ion batteries. *Energy Environ Sci* 2021;14:5669-89. DOI
24. Li C, Zhang X, Zhu Y, et al. Modulating the lithiophilicity at electrode/electrolyte interface for high-energy Li-metal batteries. *EM* 2021. DOI
25. Chang H, Wu Y, Han X, Yi T. Recent developments in advanced anode materials for lithium-ion batteries. *EM* 2021. DOI
26. Yi Z, Chen G, Hou F, Wang L, Liang J. Strategies for the stabilization of Zn metal anodes for Zn-ion batteries. *Advanced Energy Materials* 2021;11:2003065. DOI
27. He H, Qin H, Wu J, et al. Engineering interfacial layers to enable Zn metal anodes for aqueous zinc-ion batteries. *Energy Storage Materials* 2021;43:317-36. DOI
28. Dong H, Li J, Guo J, et al. Insights on flexible Zinc-ion batteries from lab research to commercialization. *Adv Mater* 2021;33:e2007548. DOI PubMed

29. Li C, Wang L, Zhang J, et al. Roadmap on the protective strategies of zinc anodes in aqueous electrolyte. *Energy Storage Materials* 2022;44:104-35. [DOI](#)
30. Yin Y, Wang S, Zhang Q, et al. Dendrite-free Zinc deposition induced by tin-modified multifunctional 3D host for stable zinc-based flow battery. *Adv Mater* 2020;32:e1906803. [DOI](#) [PubMed](#)
31. Wang SB, Ran Q, Yao RQ, et al. Lamella-nanostructured eutectic zinc-aluminum alloys as reversible and dendrite-free anodes for aqueous rechargeable batteries. *Nat Commun* 2020;11:1634. [DOI](#) [PubMed](#) [PMC](#)
32. Wippermann K, Schultze J, Kessel R, Penninger J. The inhibition of zinc corrosion by bisaminotriazole and other triazole derivatives. *Corros Sci* 1991;32:205-30. [DOI](#)
33. Cai Z, Ou Y, Wang J, et al. Chemically resistant Cu-Zn/Zn composite anode for long cycling aqueous batteries. *Energy Stor Mater* 2020;27:205-11. [DOI](#)
34. Li W, Wang K, Zhou M, Zhan H, Cheng S, Jiang K. Advanced low-cost, high-voltage, long-life aqueous hybrid sodium/zinc batteries enabled by a dendrite-free zinc anode and concentrated electrolyte. *ACS Appl Mater Interfaces* 2018;10:22059-66. [DOI](#) [PubMed](#)
35. Li Z, Wu L, Dong S, et al. Pencil drawing stable interface for reversible and durable aqueous zinc-ion batteries. *Adv Funct Mater* 2021;31:2006495. [DOI](#)
36. Du Y, Liu C, Liu Y, Han Q, Chi X, Liu Y. Carbon fiber micron film guided uniform plating/stripping of metals: a universal approach for highly stable metal batteries. *Electrochimica Acta* 2020;339:135867. [DOI](#)
37. Li M, He Q, Li Z, et al. A novel dendrite-free Mn²⁺/Zn²⁺ hybrid battery with 2.3 V voltage window and 11000-cycle lifespan. *Adv Energy Mater* 2019;9:1901469. [DOI](#)
38. Zheng J, Zhao Q, Tang T, et al. Reversible epitaxial electrodeposition of metals in battery anodes. *Science* 2019;366:645-8. [DOI](#) [PubMed](#)
39. Shen C, Li X, Li N, et al. Graphene-boosted, high-performance aqueous Zn-Ion battery. *ACS Appl Mater Interfaces* 2018;10:25446-53. [DOI](#) [PubMed](#)
40. Xia A, Pu X, Tao Y, Liu H, Wang Y. Graphene oxide spontaneous reduction and self-assembly on the zinc metal surface enabling a dendrite-free anode for long-life zinc rechargeable aqueous batteries. *Appl Surf Sci* 2019;481:852-9. [DOI](#)
41. Liu P, Liu W, Huang Y, Li P, Yan J, Liu K. Mesoporous hollow carbon spheres boosted, integrated high performance aqueous Zn-Ion energy storage. *Energy Storage Materials* 2020;25:858-65. [DOI](#)
42. Wu C, Xie K, Ren K, Yang S, Wang Q. Dendrite-free Zn anodes enabled by functional nitrogen-doped carbon protective layers for aqueous zinc-ion batteries. *Dalton Trans* 2020;49:17629-34. [DOI](#) [PubMed](#)
43. Yuksel R, Buyukcakir O, Seong WK, Ruoff RS. Metal-organic framework integrated anodes for aqueous zinc-ion batteries. *Adv Energy Mater* 2020;10:1904215. [DOI](#)
44. Zhai S, Wang N, Tan X, et al. Interface-engineered dendrite-free anode and ultraconductive cathode for durable and high-rate fiber Zn dual-ion microbattery. *Adv Funct Mater* 2021;31:2008894. [DOI](#)
45. Zhou J, Xie M, Wu F, et al. Ultrathin surface coating of nitrogen-doped graphene enables stable zinc anodes for aqueous zinc-ion batteries. *Adv Mater* 2021;33:e2101649. [DOI](#) [PubMed](#)
46. Zhang X, Li J, Liu D, et al. Ultra-long-life and highly reversible Zn metal anodes enabled by a desolvation and deanionization interface layer. *Energy Environ Sci* 2021;14:3120-9. [DOI](#)
47. Cao J, Zhang D, Zhang X, Sawangphruk M, Qin J, Liu R. A universal and facile approach to suppress dendrite formation for a Zn and Li metal anode. *J Mater Chem A* 2020;8:9331-44. [DOI](#)
48. Yang X, Li W, Lv J, et al. In situ separator modification via CVD-derived N-doped carbon for highly reversible Zn metal anodes. *Nano Res.* [DOI](#)
49. Li C, Sun Z, Yang T, et al. Directly grown vertical graphene carpets as janus separators toward stabilized Zn metal anodes. *Adv Mater* 2020;32:e2003425. [DOI](#) [PubMed](#)
50. Cao J, Zhang D, Gu C, et al. Manipulating crystallographic orientation of zinc deposition for dendrite-free zinc ion batteries. *Adv Energy Mater* 2021;11:2101299. [DOI](#)
51. Liang Y, Wang Y, Mi H, et al. Functionalized carbon nanofiber interlayer towards dendrite-free, Zn-ion batteries. *Chemical Engineering Journal* 2021;425:131862. [DOI](#)
52. Li G, Li Y, Liu H, Guo Y, Li Y, Zhu D. Architecture of graphdiyne nanoscale films. *Chem Commun (Camb)* 2010;46:3256-8. [DOI](#) [PubMed](#)
53. Li J, Chen Y, Guo J, Wang F, Liu H, Li Y. Graphdiyne oxide-based high-performance rechargeable aqueous Zn-MnO₂ battery. *Adv Funct Mater* 2020;30:2004115. [DOI](#)
54. Wang F, Xiong Z, Jin W, Liu H, Liu H. Graphdiyne oxide for aqueous zinc ion full battery with ultra-long cycling stability. *Nano Today* 2022;44:101463. [DOI](#)
55. Yang Q, Guo Y, Yan B, et al. Hydrogen-substituted graphdiyne ion tunnels directing concentration redistribution for commercial-grade dendrite-free zinc anodes. *Adv Mater* 2020;32:e2001755. [DOI](#) [PubMed](#)
56. Yang Q, Li L, Hussain T, et al. Stabilizing interface pH by N-modified graphdiyne for dendrite-free and high-rate aqueous Zn-ion batteries. *Angew Chem Int Ed Engl* 2022;61:e202112304. [DOI](#) [PubMed](#)
57. Liang P, Yi J, Liu X, et al. Highly reversible Zn anode enabled by controllable formation of nucleation sites for Zn-based batteries. *Adv Funct Mater* 2020;30:1908528. [DOI](#)
58. Cao J, Zhang D, Gu C, et al. Modulating Zn deposition via ceramic-cellulose separator with interfacial polarization effect for durable

- zinc anode. *Nano Energy* 2021;89:106322. DOI
59. Zhou M, Guo S, Fang G, et al. Suppressing by-product via stratified adsorption effect to assist highly reversible zinc anode in aqueous electrolyte. *Journal of Energy Chemistry* 2021;55:549-56. DOI
60. Jin H, Dai S, Xie K, et al. Regulating interfacial desolvation and deposition kinetics enables durable Zn anodes with ultrahigh utilization of 80. *Small* 2022;18:e2106441. DOI PubMed
61. Zhang Q, Luan J, Huang X, et al. Revealing the role of crystal orientation of protective layers for stable zinc anode. *Nat Commun* 2020;11:3961. DOI PubMed PMC
62. Liu H, Wang JG, Hua W, et al. Building ohmic contact interfaces toward ultrastable Zn metal anodes. *Adv Sci (Weinh)* 2021;8:e2102612. DOI PubMed PMC
63. Xie X, Liang S, Gao J, et al. Manipulating the ion-transfer kinetics and interface stability for high-performance zinc metal anodes. *Energy Environ Sci* 2020;13:503-10. DOI
64. Han X, Leng H, Qi Y, et al. Hydrophilic silica spheres layer as ions shunt for enhanced Zn metal anode. *Chemical Engineering Journal* 2022;431:133931. DOI
65. Zhou X, Cao P, Wei A, et al. Driving the interfacial ion-transfer kinetics by mesoporous TiO₂ spheres for high-performance aqueous Zn-ion batteries. *ACS Appl Mater Interfaces* 2021;13:8181-90. DOI PubMed
66. Zhao K, Wang C, Yu Y, et al. Ultrathin surface coating enables stabilized zinc metal Anode. *Adv Mater Interfaces* 2018;5:1800848. DOI
67. He H, Tong H, Song X, Song X, Liu J. Highly stable Zn metal anodes enabled by atomic layer deposited Al₂O₃ coating for aqueous zinc-ion batteries. *J Mater Chem A* 2020;8:7836-46. DOI
68. Hao J, Li B, Li X, et al. An in-depth study of zn metal surface chemistry for advanced aqueous zn-ion batteries. *Adv Mater* 2020;32:e2003021. DOI PubMed
69. Bhojate S, Mhin S, Jeon JE, Park K, Kim J, Choi W. Stable and high-energy-density Zn-ion rechargeable batteries based on a MoS₂-coated Zn anode. *ACS Appl Mater Interfaces* 2020;12:27249-57. DOI PubMed
70. Jia H, Qiu M, Lan C, et al. Advanced Zinc anode with nitrogen-doping interface induced by plasma surface treatment. *Adv Sci (Weinh)* 2022;9:e2103952. DOI PubMed PMC
71. Zheng J, Cao Z, Ming F, et al. Preferred orientation of TiN coatings enables stable zinc anodes. *ACS Energy Lett* 2022;7:197-203. DOI
72. Yang Z, Lv C, Li W, et al. Revealing the two-dimensional surface diffusion mechanism for zinc dendrite formation on zinc anode. *Small* 2021:e2104148. DOI PubMed
73. Ma L, Li Q, Ying Y, et al. Toward practical high-areal-capacity aqueous zinc-metal batteries: quantifying hydrogen evolution and a solid-ion conductor for stable zinc anodes. *Adv Mater* 2021;33:e2007406. DOI PubMed
74. Yang Y, Liu C, Lv Z, et al. Synergistic manipulation of Zn²⁺ ion flux and desolvation effect enabled by anodic growth of a 3D ZnF₂ matrix for long-lifespan and dendrite-free Zn metal anodes. *Adv Mater* 2021;33:e2007388. DOI PubMed
75. Han J, Euchner H, Kuenzel M, et al. A thin and uniform fluoride-based artificial interphase for the zinc metal anode enabling reversible Zn/MnO₂ batteries. *ACS Energy Lett* 2021;6:3063-71. DOI
76. Liang G, Zhu J, Yan B, et al. Gradient fluorinated alloy to enable highly reversible Zn-metal anode chemistry. *Energy Environ Sci* 2022;15:1086-96. DOI
77. Cao P, Zhou X, Wei A, et al. Fast-charging and ultrahigh-capacity zinc metal anode for high-performance aqueous zinc-ion batteries. *Adv Funct Mater* 2021;31:2100398. DOI
78. Peng H, Liu C, Wang N, et al. Intercalation of organics into layered structures enables superior interface compatibility and fast charge diffusion for dendrite-free Zn anodes. *Energy Environ Sci* 2022;15:1682-93. DOI
79. Hong L, Wu X, Ma C, et al. Boosting the Zn-ion transfer kinetics to stabilize the Zn metal interface for high-performance rechargeable Zn-ion batteries. *J Mater Chem A* 2021;9:16814-23. DOI
80. Yang Y, Liu C, Lv Z, et al. Redistributing Zn-ion flux by interlayer ion channels in Mg-Al layered double hydroxide-based artificial solid electrolyte interface for ultra-stable and dendrite-free Zn metal anodes. *Energy Storage Materials* 2021;41:230-9. DOI
81. Liu M, Cai J, Ao H, Hou Z, Zhu Y, Qian Y. NaTi₂(PO₄)₃ Solid-state electrolyte protection layer on Zn metal anode for superior long-life aqueous zinc-ion batteries. *Adv Funct Mater* 2020;30:2004885. DOI
82. Xiao P, Xue L, Guo Y, et al. On-site building of a Zn²⁺-conductive interfacial layer via short-circuit energization for stable Zn anode. *Science Bulletin* 2021;66:545-52. DOI
83. Kang L, Cui M, Jiang F, et al. Nanoporous CaCO₃ coatings enabled uniform Zn stripping/plating for long-life zinc rechargeable aqueous batteries. *Adv Energy Mater* 2018;8:1801090. DOI
84. Wu K, Yi J, Liu X, et al. Regulating Zn deposition via an artificial solid-electrolyte interface with aligned dipoles for long life Zn anode. *Nanomicro Lett* 2021;13:79. DOI PubMed PMC
85. Zou P, Zhang R, Yao L, et al. Ultrahigh-rate and long-life zinc-metal anodes enabled by self-accelerated cation migration. *Adv Energy Mater* 2021;11:2100982. DOI
86. Chen A, Zhao C, Guo Z, et al. Fast-growing multifunctional ZnMoO₄ protection layer enable dendrite-free and hydrogen-suppressed Zn anode. *Energy Storage Materials* 2022;44:353-9. DOI
87. Ma C, Wang X, Lu W, et al. Achieving stable Zn metal anode via a simple NiCo layered double hydroxides artificial coating for high performance aqueous Zn-ion batteries. *Chemical Engineering Journal* 2022;429:132576. DOI

88. Su XH, Han CX, Zhang J, Wang ZJ. Preparation and electrochemical performance of CoNiO₂/Ti₃C₂T_x composites. *J Chin Ceram Soc* 2021;49:1033-1040. DOI: 10.14062/j.issn.0454.
89. Chang C, Chen W, Chen Y, et al. Recent progress on two-dimensional materials. *Acta Physico Chimica Sinica* 2021;0:2108017-0. DOI
90. Zhang N, Huang S, Yuan Z, Zhu J, Zhao Z, Niu Z. Direct self-assembly of mxene on Zn anodes for dendrite-free aqueous zinc-ion batteries. *Angew Chem Int Ed Engl* 2021;60:2861-5. DOI PubMed
91. Sun C, Wu C, Gu X, Wang C, Wang Q. Interface engineering via Ti₃C₂T_x mxene electrolyte additive toward dendrite-free zinc deposition. *Nanomicro Lett* 2021;13:89. DOI PubMed PMC
92. Li X, Li M, Luo K, et al. Lattice matching and halogen regulation for synergistically induced uniform zinc electrodeposition by halogenated Ti₃C₂ mxenes. *ACS Nano* ;2021:813-22. DOI PubMed
93. Zou K, Cai P, Deng X, et al. Highly stable zinc metal anode enabled by oxygen functional groups for advanced Zn-ion supercapacitors. *Chem Commun* 2021;57:528-31. DOI
94. Li Z, Deng W, Li C, et al. Uniformizing the electric field distribution and ion migration during zinc plating/stripping. *via* ;8:17725-31. DOI
95. Jiao S, Fu J, Wu M, Hua T, Hu H. Ion sieve: tailoring Zn²⁺ desolvation kinetics and flux toward dendrite-free metallic zinc anodes. *ACS Nano* ;2021:1013-24. DOI PubMed
96. Du H, Zhao R, Yang Y, Liu Z, Qie L, Huang Y. High-capacity and long-life zinc electrodeposition enabled by a self-healable and desolvation shield for aqueous zinc-ion batteries. *Angew Chem Int Ed Engl* 2022;61:e202114789. DOI PubMed
97. Jiao Y, Li F, Jin X, et al. Engineering polymer glue towards 90% zinc utilization for 1000 hours to make high-performance zn-ion batteries. *Adv Funct Mater* 2021;31:2107652. DOI
98. Lee D, Kim H, Kim W, et al. Water-repellent ionic liquid skinny gels customized for aqueous Zn-Ion battery anodes. *Adv Funct Mater* 2021;31:2103850. DOI
99. Zou P, Nykypanchuk D, Doerk G, Xin HL. Hydrophobic molecule monolayer brush-tethered zinc anodes for aqueous zinc batteries. *ACS Appl Mater Interfaces* 2021;13:60092-8. DOI PubMed
100. Hieu LT, So S, Kim IT, Hur J. Zn anode with flexible β-PVDF coating for aqueous Zn-ion batteries with long cycle life. *Chemical Engineering Journal* 2021;411:128584. DOI
101. Wang Y, Guo T, Yin J, et al. Controlled deposition of zinc-metal anodes via selectively polarized ferroelectric polymers. *Adv Mater* 2022;34:e2106937. DOI PubMed
102. Zhao Z, Zhao J, Hu Z, et al. Long-life and deeply rechargeable aqueous Zn anodes enabled by a multifunctional brightener-inspired interphase. *Energy Environ Sci* 2019;12:1938-49. DOI
103. Chen P, Zhou W, Xiao Z, et al. An integrated configuration with robust interfacial contact for durable and flexible zinc ion batteries. *Nano Energy* 2020;74:104905. DOI
104. Cao Z, Zhu X, Xu D, et al. Eliminating Zn dendrites by commercial cyanoacrylate adhesive for zinc ion battery. *Energy Storage Materials* 2021;36:132-8. DOI
105. Park SH, Byeon SY, Park J, Kim C. Insight into the critical role of surface hydrophilicity for dendrite-free zinc metal anodes. *ACS Energy Lett* 2021;6:3078-85. DOI
106. Kim S, Yang X, Cho M, Lee Y. Nanostructured conductive polymer shield for highly reversible dendrite-free zinc metal anode. *Chem Eng J* 2022;427:131954. DOI
107. Chen P, Yuan X, Xia Y, et al. An artificial polyacrylonitrile coating layer confining zinc dendrite growth for highly reversible aqueous zinc-based batteries. *Adv Sci (Weinh)* 2021;8:e2100309. DOI PubMed PMC
108. Liu P, Zhang Z, Hao R, et al. Ultra-highly stable zinc metal anode via 3D-printed g-C₃N₄ modulating interface for long life energy storage systems. *Chem Eng J* 2021;403:126425. DOI
109. Park JH, Kwak MJ, Hwang C, et al. Self-assembling films of covalent organic frameworks enable long-term, efficient cycling of zinc-ion batteries. *Adv Mater* 2021;33:e2101726. DOI PubMed
110. Zhao Z, Wang R, Peng C, et al. Horizontally arranged zinc platelet electrodeposits modulated by fluorinated covalent organic framework film for high-rate and durable aqueous zinc ion batteries. *Nat Commun* 2021;12:6606. DOI PubMed PMC
111. Zhao J, Ying Y, Wang G, et al. Covalent organic framework film protected zinc anode for highly stable rechargeable aqueous zinc-ion batteries. *Energy Storage Materials* 2022;48:82-9. DOI
112. Ding J, Liu Y, Huang S, et al. In Situ construction of a multifunctional quasi-gel layer for long-life aqueous zinc metal anodes. *ACS Appl Mater Interfaces* 2021;13:29746-54. DOI PubMed
113. Zhu M, Hu J, Lu Q, et al. A patternable and in situ formed polymeric zinc blanket for a reversible zinc anode in a skin-mountable microbattery. *Adv Mater* 2021;33:e2007497. DOI PubMed
114. Shin J, Lee J, Kim Y, Park Y, Kim M, Choi JW. Highly reversible, grain-directed zinc deposition in aqueous zinc-ion batteries. *Adv Energy Mater* 2021;11:2100676. DOI
115. Liu M, Yang L, Liu H, et al. Artificial solid-electrolyte interface facilitating dendrite-free zinc metal anodes via nanowetting effect. *ACS Appl Mater Interfaces* 2019;11:32046-51. DOI PubMed
116. Yang H, Chang Z, Qiao Y, et al. Constructing a super-saturated electrolyte front surface for stable rechargeable aqueous zinc batteries. *Angew Chem Int Ed Engl* 2020;59:9377-81. DOI PubMed
117. He M, Shu C, Hu A, et al. Suppressing dendrite growth and side reactions on Zn metal anode via guiding interfacial

- anion/cation/H₂O distribution by artificial multi-functional interface layer. *Energy Storage Materials* 2022;44:452-60. DOI
118. Li G. Regulating mass transport behavior for high-performance lithium metal batteries and fast-charging lithium-ion batteries. *Adv Energy Mater* 2021;11:2002891. DOI
 119. Yuan D, Manalastas W Jr, Zhang L, et al. Lignin@Nafion membranes forming Zn solid-electrolyte interfaces enhance the cycle life for rechargeable zinc-ion batteries. *ChemSusChem* 2019;12:4889-900. DOI PubMed
 120. Wu B, Wu Y, Lu Z, et al. A cation selective separator induced cathode protective layer and regulated zinc deposition for zinc ion batteries. *J Mater Chem A* 2021;9:4734-43. DOI
 121. Fang Y, Xie X, Zhang B, et al. Regulating zinc deposition behaviors by the conditioner of PAN separator for zinc-ion batteries. *Adv Funct Materials* 2022;32:2109671. DOI
 122. Lee BS, Cui S, Xing X, et al. Dendrite suppression membranes for rechargeable zinc batteries. *ACS Appl Mater Interfaces* 2018;10:38928-35. DOI PubMed
 123. Zhi J, Li S, Han M, Chen P. Biomolecule-guided cation regulation for dendrite-free metal anodes. *Sci Adv* 2020;6:eabb1342. DOI PubMed PMC
 124. Wu L, Zhang Y, Shang P, Dong Y, Wu Z. Redistributing Zn ion flux by bifunctional graphitic carbon nitride nanosheets for dendrite-free zinc metal anodes. *J Mater Chem A* 2021;9:27408-14. DOI
 125. Liu T, Hong J, Wang J, Xu Y, Wang Y. Uniform distribution of zinc ions achieved by functional supramolecules for stable zinc metal anode with long cycling lifespan. *Energy Storage Materials* 2022;45:1074-83. DOI
 126. Wang Z, Dong L, Huang W, et al. Simultaneously regulating uniform Zn²⁺ flux and electron conduction by MOF/rGO interlayers for high-performance Zn anodes. *Nanomicro Lett* 2021;13:73. DOI PubMed PMC
 127. Yang H, Qiao Y, Chang Z, Deng H, He P, Zhou H. A metal-organic framework as a multifunctional ionic sieve membrane for long-life aqueous zinc-iodide batteries. *Adv Mater* 2020;32:e2004240. DOI PubMed
 128. Zhang L, Zhang B, Zhang T, et al. Eliminating dendrites and side reactions via a multifunctional ZnSe protective layer toward advanced aqueous Zn metal batteries. *Adv Funct Materials* 2021;31:2100186. DOI
 129. Li TC, Lim YV, Xie X, et al. ZnSe Modified zinc metal anodes: toward enhanced zincophilicity and ionic diffusion. *Small* 2021;17:e2101728. DOI PubMed
 130. Yang X, Li C, Sun Z, et al. Interfacial manipulation via in situ grown ZnSe cultivator toward highly reversible Zn metal anodes. *Adv Mater* 2021;33:e2105951. DOI PubMed
 131. Cao P, Tang J, Wei A, et al. Manipulating uniform nucleation to achieve dendrite-free Zn anodes for aqueous Zn-ion batteries. *ACS Appl Mater Interfaces* 2021;13:48855-64. DOI PubMed
 132. Cui M, Xiao Y, Kang L, et al. Quasi-isolated Au particles as heterogeneous seeds to guide uniform Zn deposition for aqueous zinc-ion batteries. *ACS Appl Energy Mater* 2019;2:6490-6. DOI
 133. Li Z, Gong Z, Wu X, et al. Dendrite-free and anti-corrosion Zn metal anode enabled by an artificial layer for high-performance Zn ion capacitor. *Chin Chem Lett* 2021. DOI
 134. Han D, Wu S, Zhang S, et al. A corrosion-resistant and dendrite-free zinc metal anode in aqueous systems. *Small* 2020;16:e2001736. DOI PubMed
 135. Cai Z, Ou Y, Zhang B, et al. A replacement reaction enabled interdigitated metal/solid electrolyte architecture for battery cycling at 20 mA cm⁻² and 20 mAh cm⁻². *J Am Chem Soc* 2021;143:3143-52. DOI PubMed
 136. Hu K, Guan X, Lv R, et al. Stabilizing zinc metal anodes by artificial solid electrolyte interphase through a surface ion-exchanging strategy. *Chem Eng J* 2020;396:125363. DOI
 137. Hong L, Wang LY, Wang Y, et al. Toward hydrogen-free and dendrite-free aqueous zinc batteries: formation of zincophilic protective layer on Zn anodes. *Adv Sci (Weinh)* 2022;9:e2104866. DOI PubMed PMC
 138. Zhang Y, Wang G, Yu F, et al. Highly reversible and dendrite-free Zn electrodeposition enabled by a thin metallic interfacial layer in aqueous batteries. *Chem Eng J* 2021;416:128062. DOI
 139. Wang Y, Chen Y, Liu W, et al. Uniform and dendrite-free zinc deposition enabled by *in situ*. *in situ*;9:8452-61. DOI
 140. Lu Q, Liu C, Du Y, et al. Uniform Zn deposition achieved by Ag coating for improved aqueous zinc-ion batteries. *ACS Appl Mater Interfaces* 2021;13:16869-75. DOI PubMed
 141. Liu C, Luo Z, Deng W, et al. Liquid alloy interlayer for aqueous zinc-ion battery. *ACS Energy Lett* 2021;6:675-83. DOI
 142. Jia H, Wang Z, Dirican M, et al. A liquid metal assisted dendrite-free anode for high-performance Zn-ion batteries. *J Mater Chem A* 2021;9:5597-605. DOI
 143. Gu J, Tao Y, Chen H, et al. Stress-release functional liquid metal-mxene layers toward dendrite-free zinc metal anodes. *Advanced Energy Materials*. DOI
 144. Liu C, Lu Q, Omar A, Mikhailova D. A facile chemical method enabling uniform Zn deposition for improved aqueous Zn-ion batteries. *Nanomaterials (Basel)* 2021;11:764. DOI PubMed PMC
 145. Xie S, Li Y, Li X, et al. Stable zinc anodes enabled by zincophilic Cu nanowire networks. *Nanomicro Lett* 2021;14:39. DOI PubMed PMC
 146. Li S, Fu J, Miao G, et al. Toward planar and dendrite-free Zn electrodepositions by regulating Sn-crystal textured surface. *Adv Mater* 2021;33:e2008424. DOI PubMed
 147. Guo W, Zhang Y, Tong X, et al. Multifunctional tin layer enabled long-life and stable anode for aqueous zinc-ion batteries. *Materials Today Energy* 2021;20:100675. DOI

148. Huang Y, Chang Z, Liu W, et al. Layer-by-layer zinc metal anodes to achieve long-life zinc-ion batteries. *Chem Eng J* 2022;431:133902. [DOI](#)
149. Zhao R, Yang Y, Liu G, et al. Redirected Zn Electrodeposition by an Anti-Corrosion Elastic Constraint for Highly Reversible Zn Anodes. *Adv Funct Mater* 2021;31:2001867. [DOI](#)
150. Cui Y, Zhao Q, Wu X, et al. An interface-bridged organic-inorganic layer that suppresses dendrite formation and side reactions for ultra-long-life aqueous zinc metal anodes. *Angew Chem Int Ed Engl* 2020;59:16594-601. [DOI](#) [PubMed](#)
151. He H, Liu J. Suppressing Zn dendrite growth by molecular layer deposition to enable long-life and deeply rechargeable aqueous Zn anodes. *J Mater Chem A* 2020;8:22100-10. [DOI](#)
152. Zhou S, Wang Y, Lu H, et al. Anti-corrosive and Zn-ion-regulating composite interlayer enabling long-life Zn metal anodes. *Adv Funct Materials* 2021;31:2104361. [DOI](#)
153. Guo Z, Fan L, Zhao C, et al. A dynamic and self-adapting interface coating for stable Zn-metal anodes. *Adv Mater* 2022;34:e2105133. [DOI](#) [PubMed](#)
154. Di S, Nie X, Ma G, et al. Zinc anode stabilized by an organic-inorganic hybrid solid electrolyte interphase. *Energy Storage Materials* 2021;43:375-82. [DOI](#)
155. Wu S, Zhang S, Chu Y, Hu Z, Luo J. Stacked lamellar matrix enabling regulated deposition and superior thermo-kinetics for advanced aqueous Zn-ion system under practical conditions. *Adv Funct Mater* 2021;31:2107397. [DOI](#)
156. Zhang Y, Zhu M, Wang G, et al. Dendrites-free Zn metal anodes enabled by an artificial protective layer filled with 2D anionic nanosheets. *Small Methods* 2021;5:e2100650. [DOI](#) [PubMed](#)
157. Xu X, Chen Y, Zheng D, et al. Ultra-fast and scalable saline immersion strategy enabling uniform Zn nucleation and deposition for high-performance Zn-ion batteries. *Small* 2021;17:e2101901. [DOI](#) [PubMed](#)
158. Mu Y, Zhou T, Li D, et al. Highly stable and durable Zn-metal anode coated by bi-functional protective layer suppressing uncontrollable dendrites growth and corrosion. *Chem Eng J* 2022;430:132839. [DOI](#)
159. An Y, Tian Y, Liu C, Xiong S, Feng J, Qian Y. Rational design of sulfur-doped three-dimensional $Ti_3C_2T_x$. *Small* 2021;15:15259-73. [DOI](#) [PubMed](#)
160. Deng W, Zhang N, Wang X. Hybrid interlayer enables dendrite-free and deposition-modulated zinc anodes. *Chem Eng J* 2022;432:134378. [DOI](#)
161. Feng G, Guo J, Tian H, et al. Probe the localized electrochemical environment effects and electrode reaction dynamics for metal batteries using in situ 3D microscopy. *Adv Energy Mater* 2022;12:2103484. [DOI](#)
162. Cui B, Han X, Hu W. Micronanostructured design of dendrite-free zinc anodes and their applications in aqueous zinc-based rechargeable batteries. *Small Structures* 2021;2:2000128. [DOI](#)
163. Wang J, Cai Z, Xiao R, et al. A chemically polished zinc metal electrode with a ridge-like structure for cycle-stable aqueous batteries. *ACS Appl Mater Interfaces* 2020;12:23028-34. [DOI](#) [PubMed](#)
164. Xu Y, Wang C, Shi Y, Miao G, Fu J, Huang Y. A self-preserving pitted texture enables reversible topographic evolution and cycling on Zn metal anodes. *J Mater Chem A* 2021;9:25495-501. [DOI](#)
165. Zhang Y, Han X, Liu R, et al. Manipulating the zinc deposition behavior in hexagonal patterns at the preferential Zn (100) crystal plane to construct surficial dendrite-free zinc metal anode. *Small* 2022;18:e2105978. [DOI](#) [PubMed](#)
166. Wang W, Huang G, Wang Y, et al. Organic acid etching strategy for dendrite suppression in aqueous zinc-ion batteries. *Advanced Energy Materials* 2022;12:2102797. [DOI](#)
167. Wang X, Meng J, Lin X, et al. Stable zinc metal anodes with textured crystal faces and functional zinc compound coatings. *Adv Funct Materials* 2021;31:2106114. [DOI](#)
168. Zhou M, Guo S, Li J, et al. Surface-preferred crystal plane for a stable and reversible zinc anode. *Adv Mater* 2021;33:e2100187. [DOI](#) [PubMed](#)
169. Zheng J, Deng Y, Yin J, et al. Textured electrodes: manipulating built-in crystallographic heterogeneity of metal electrodes via severe plastic deformation. *Adv Mater* 2022;34:e2106867. [DOI](#) [PubMed](#)
170. Wang J, Zhang B, Cai Z, et al. Stable interphase chemistry of textured Zn anode for rechargeable aqueous batteries. *Science Bulletin* 2022;67:716-24. [DOI](#)
171. Chen K, Guo H, Li W, Wang Y. Dual porous 3D zinc anodes toward dendrite-free and long cycle life zinc-ion batteries. *ACS Appl Mater Interfaces* 2021;13:54990-6. [DOI](#) [PubMed](#)
172. Liu H, Li J, Zhang X, et al. Ultrathin and ultralight Zn micromesh-induced spatial-selection deposition for flexible high-specific-energy Zn-ion batteries. *Adv Funct Materials* 2021;31:2106550. [DOI](#)
173. Xiao R, Cai Z, Zhan R, et al. Localizing concentrated electrolyte in pore geometry for highly reversible aqueous Zn metal batteries. *Chem Eng J* 2021;420:129642. [DOI](#)
174. Li C, Shi X, Liang S, et al. Spatially homogeneous copper foam as surface dendrite-free host for zinc metal anode. *Chem Eng J* 2020;379:122248. [DOI](#)
175. Zhang Q, Luan J, Huang X, et al. Simultaneously regulating the ion distribution and electric field to achieve dendrite-free Zn anode. *Small* 2020;16:e2000929. [DOI](#) [PubMed](#)
176. Zeng Y, Sun PX, Pei Z, et al. Nitrogen-doped carbon fibers embedded with zincophilic Cu nanoboxes for stable Zn-metal anodes. *Adv Mater* 2022:e2200342. [DOI](#) [PubMed](#)
177. An Y, Tian Y, Xiong S, Feng J, Qian Y. Scalable and controllable synthesis of interface-engineered nanoporous host for dendrite-free

- and high rate zinc metal batteries. *ACS Nano* ;2021:11828-42. DOI PubMed
178. Zhang G, Zhang X, Liu H, Li J, Chen Y, Duan H. 3D-printed multi-channel metal lattices enabling localized electric-field redistribution for dendrite-free aqueous Zn-ion batteries. *Adv Energy Mater* 2021;11:2003927. DOI
179. Shen Z, Luo L, Li C, et al. Stratified zinc-binding strategy toward prolonged cycling and flexibility of aqueous fibrous zinc metal batteries. *Adv Energy Mater* 2021;11:2100214. DOI
180. Jian Q, Guo Z, Zhang L, Wu M, Zhao T. A hierarchical porous tin host for dendrite-free, highly reversible zinc anodes. *Chem Eng J* 2021;425:130643. DOI
181. Qian Y, Meng C, He J, Dong X. A lightweight 3D Zn@Cu nanosheets@activated carbon cloth as long-life anode with large capacity for flexible zinc ion batteries. *Journal of Power Sources* 2020;480:228871. DOI
182. Zeng Y, Zhang X, Qin R, et al. Dendrite-free zinc deposition induced by multifunctional CNT frameworks for stable flexible Zn-ion batteries. *Adv Mater* 2019;31:e1903675. DOI PubMed
183. Chen T, Wang Y, Yang Y, et al. Heterometallic seed-mediated zinc deposition on inkjet printed silver nanoparticles toward foldable and heat-resistant zinc batteries. *Adv Funct Mater* 2021;31:2101607. DOI
184. Zheng J, Bock DC, Tang T, et al. Regulating electrodeposition morphology in high-capacity aluminium and zinc battery anodes using interfacial metal-substrate bonding. *Nat Energy* 2021;6:398-406. DOI
185. Hong C, Yang G, Wang C. Highly reversible Zn electrodeposition enabled by an artificial 3D defect-rich conductive scaffold. *ACS Appl Mater Interfaces* 2021;13:54088-95. DOI PubMed
186. Xie F, Li H, Wang X, et al. Mechanism for zincophilic sites on zinc-metal anode hosts in aqueous batteries. *Adv Energy Mater* 2021;11:2003419. DOI
187. Wan F, Hao Z, Wang S, et al. A Universal compensation strategy to anchor polar organic molecules in bilayered hydrated vanadates for promoting aqueous zinc-ion storage. *Adv Mater* 2021;33:e2102701. DOI PubMed
188. Cao Q, Gao H, Gao Y, et al. Regulating dendrite-free zinc deposition by 3D zincophilic nitrogen-doped vertical graphene for high-performance flexible Zn-ion batteries. *Adv Funct Mater* 2021;31:2103922. DOI
189. Tian Y, An Y, Wei C, et al. Flexible and free-standing Ti₃C₂T_x. *ACS Nano* 2021;13:11676-85. DOI PubMed
190. Tian Y, An Y, Liu C, Xiong S, Feng J, Qian Y. Reversible zinc-based anodes enabled by zincophilic antimony engineered MXene for stable and dendrite-free aqueous zinc batteries. *Energy Storage Materials* 2021;41:343-53. DOI
191. Zhou J, Xie M, Wu F, et al. Encapsulation of metallic Zn in a hybrid mxene/graphene aerogel as a stable Zn anode for foldable Zn-ion batteries. *Adv Mater* 2022;34:e2106897. DOI PubMed
192. Wang Z, Huang J, Guo Z, et al. A metal-organic framework host for highly reversible dendrite-free zinc metal anodes. *Joule* 2019;3:1289-300. DOI
193. Sun PX, Cao Z, Zeng YX, et al. Formation of super-assembled TiO_x/Zn/N-doped carbon inverse opal towards dendrite-free Zn anodes. *Angew Chem Int Ed Engl* 2022;61:e202115649. DOI PubMed
194. Zhang Y, Howe JD, Ben-yoseph S, Wu Y, Liu N. Unveiling the origin of alloy-seeded and nondendritic growth of Zn for rechargeable aqueous Zn batteries. *ACS Energy Lett* 2021;6:404-12. DOI
195. Tian H, Li Z, Feng G, et al. Stable, high-performance, dendrite-free, seawater-based aqueous batteries. *Nat Commun* 2021;12:237. DOI PubMed PMC
196. Wang L, Huang W, Guo W, et al. Sn alloying to inhibit hydrogen evolution of Zn metal anode in rechargeable aqueous batteries. *Adv Funct Materials* 2022;32:2108533. DOI
197. Zhou L, Yang F, Zeng S, et al. Zincophilic Cu sites induce dendrite-free Zn anodes for robust alkaline/neutral aqueous batteries. *Adv Funct Materials* 2022;32:2110829. DOI
198. Wan F, Wang X, Bi S, Niu Z, Chen J. Freestanding reduced graphene oxide/sodium vanadate composite films for flexible aqueous zinc-ion batteries. *Sci China Chem* 2019;62:609-15. DOI
199. Olbasa BW, Fenta FW, Chiu S, et al. High-rate and long-cycle stability with a dendrite-free zinc anode in an aqueous Zn-ion battery using concentrated electrolytes. *ACS Appl Energy Mater* 2020;3:4499-508. DOI
200. Liu Z, Yang Y, Liang S, Lu B, Zhou J. pH-buffer contained electrolyte for self-adjusted cathode-free Zn-MnO₂ batteries with coexistence of dual mechanisms. *Small Structures* 2021;2:2100119. DOI
201. Chuai M, Yang J, Wang M, et al. High-performance Zn battery with transition metal ions co-regulated electrolytic MnO₂. *eScience* 2021;1:178-85. DOI
202. Du M, Zhang F, Zhang X, et al. Calcium ion pinned vanadium oxide cathode for high-capacity and long-life aqueous rechargeable zinc-ion batteries. *Sci China Chem* 2020;63:1767-76. DOI
203. Song X, He H, Aboonahr Shiraz MH, Zhu H, Khosrozadeh A, Liu J. Enhanced reversibility and electrochemical window of Zn-ion batteries with an acetonitrile/water-in-salt electrolyte. *Chem Commun (Camb)* 2021;57:1246-9. DOI PubMed
204. Luo LW, Zhang C, Wu X, et al. A Zn-S aqueous primary battery with high energy and flat discharge plateau. *Chem Commun (Camb)* 2021;57:9918-21. DOI PubMed
205. Sun T, Yuan X, Wang K, et al. An ultralow-temperature aqueous zinc-ion battery. *J Mater Chem A* 2021;9:7042-7. DOI
206. Wang L, Zhang Y, Hu H, et al. A Zn(ClO₄)₂ electrolyte enabling long-life zinc metal electrodes for rechargeable aqueous zinc Batteries. *ACS Appl Mater Interfaces* 2019;11:42000-5. DOI PubMed
207. Kasiri G, Trócoli R, Bani Hashemi A, La Mantia F. An electrochemical investigation of the aging of copper hexacyanoferrate during the operation in zinc-ion batteries. *Electrochimica Acta* 2016;222:74-83. DOI

208. Zhang N, Cheng F, Liu Y, et al. Cation-deficient spinel ZnMn_2O_4 cathode in $\text{Zn}(\text{CF}_3\text{SO}_3)_2$ electrolyte for rechargeable aqueous Zn-ion battery. *J Am Chem Soc* 2016;138:12894-901. DOI PubMed
209. Zhang Q, Xia K, Ma Y, et al. Chaotropic anion and fast-kinetics cathode enabling low-temperature aqueous Zn batteries. *ACS Energy Lett* 2021;6:2704-12. DOI
210. Zhang Y, Zhao L, Liang Y, Wang X, Yao Y. Effect of electrolyte anions on the cycle life of a polymer electrode in aqueous batteries. *eScience* 2022. DOI
211. Huang Y, Gu Q, Guo Z, et al. Unraveling dynamical behaviors of zinc metal electrodes in aqueous electrolytes through an operando study. *Energy Storage Materials* 2022;46:243-51. DOI
212. Yuan D, Zhao J, Ren H, et al. Anion texturing towards dendrite-free Zn anode for aqueous rechargeable batteries. *Angew Chem Int Ed Engl* 2021;60:7213-9. DOI PubMed
213. Polu AR, Kumar R, Joshi GM. Effect of zinc salt on transport, structural, and thermal properties of PEG-based polymer electrolytes for battery application. *Ionics* 2014;20:675-9. DOI
214. Karan S, Sahu TB, Sahu M, Agrawal R. Investigations on Ion Transport Behaviour in a Non-Lithium Chemical Based Solid Polymer Electrolyte (SPE): [PEO:ZnA]. *Materials Today: Proceedings* 2016;3:109-14.
215. Wang W, Zhao L, Yan B, Tan X, Qi Y, He B. Effects of concentration and freeze-thaw on the first hydration shell structure of Zn^{2+} ions. *Trans Tianjin Univ* 2011;17:381-5. DOI
216. Zhang C, Holoubek J, Wu X, et al. A ZnCl_2 water-in-salt electrolyte for a reversible Zn metal anode. *Chem Commun (Camb)* 2018;54:14097-9. DOI PubMed
217. Zhang L, Rodríguez-pérez IA, Jiang H, et al. ZnCl_2 “water-in-salt” electrolyte transforms the performance of vanadium oxide as a Zn battery cathode. *Adv Funct Mater* 2019;29:1902653. DOI
218. Tang X, Wang P, Bai M, et al. Unveiling the reversibility and stability origin of the aqueous V_2O_5 -Zn batteries with a ZnCl_2 “water-in-salt” electrolyte. *Adv Sci (Weinh)* 2021;8:e2102053. DOI PubMed PMC
219. Wu X, Xu Y, Zhang C, et al. Reverse dual-ion battery via a ZnCl_2 water-in-salt electrolyte. *J Am Chem Soc* 2019;141:6338-44. DOI PubMed
220. Dong Y, Jia M, Wang Y, et al. Long-life zinc/vanadium pentoxide battery enabled by a concentrated aqueous ZnSO_4 electrolyte with proton and zinc ion Co-intercalation. *ACS Appl Energy Mater* 2020;3:11183-92. DOI
221. Patil N, Cruz C, Ciurduc D, Mavrandonakis A, Palma J, Marcilla R. An ultrahigh performance zinc-organic battery using poly(catechol) cathode in $\text{Zn}(\text{TFSI})_2$ -based concentrated aqueous electrolytes. *Adv Energy Mater* 2021;11:2100939. DOI
222. Olbasa BW, Huang C, Fenta FW, et al. Highly reversible Zn metal anode stabilized by dense and anion-derived passivation layer obtained from concentrated hybrid aqueous electrolyte. *Adv Funct Materials* 2022;32:2103959. DOI
223. Huang J, Chi X, Wu J, Liu J, Liu Y. High-concentration dual-complex electrolyte enabled a neutral aqueous zinc-manganese electrolytic battery with superior stability. *Chem Eng J* 2022;430:133058. DOI
224. Ao H, Zhu W, Liu M, et al. High-voltage and super-stable aqueous sodium-zinc hybrid ion batteries enabled by double solvation structures in concentrated electrolyte. *Small Methods* 2021;5:e2100418. DOI PubMed
225. Wang F, Borodin O, Gao T, et al. Highly reversible zinc metal anode for aqueous batteries. *Nat Mater* 2018;17:543-9. DOI PubMed
226. Zhang Y, Wan G, Lewis NHC, et al. Water or anion? *ACS Energy Lett* 2021;6:3458-63. DOI
227. Chen S, Lan R, Humphreys J, Tao S. Salt-concentrated acetate electrolytes for a high voltage aqueous Zn/MnO₂ battery. *Energy Storage Materials* 2020;28:205-15. DOI
228. Wan F, Zhang L, Dai X, Wang X, Niu Z, Chen J. Aqueous rechargeable zinc/sodium vanadate batteries with enhanced performance from simultaneous insertion of dual carriers. *Nat Commun* 2018;9:1656. DOI PubMed PMC
229. Guo X, Zhang Z, Li J, et al. Alleviation of dendrite formation on zinc anodes via electrolyte additives. *ACS Energy Lett* 2021;6:395-403. DOI
230. Zhu M, Wang X, Tang H, et al. Antifreezing hydrogel with high zinc reversibility for flexible and durable aqueous batteries by cooperative hydrated cations. *Adv Funct Mater* 2019;30:1907218. DOI
231. Wu H, Gu X, Huang P, et al. Polyoxometalate driven dendrite-free zinc electrodes with synergistic effects of cation and anion cluster regulation. *J Mater Chem A* 2021;9:7025-33. DOI
232. Jian Q, Wu M, Jiang H, Lin Y, Zhao T. A trifunctional electrolyte for high-performance zinc-iodine flow batteries. *J Power Sources* 2021;484:229238. DOI
233. Han D, Wang Z, Lu H, et al. A self-regulated interface toward highly reversible aqueous zinc batteries. *Adv Energy Mater* 2022;12:2102982. DOI
234. Li Y, Wu P, Zhong W, et al. A progressive nucleation mechanism enables stable zinc stripping–plating behavior. *Energy Environ Sci* 2021;14:5563-71. DOI
235. Yuan W, Ma G, Nie X, et al. In-situ construction of a hydroxide-based solid electrolyte interphase for robust zinc anodes. *Chem Eng J* 2022;431:134076. DOI
236. Xiao Y, Xu R, Xu L, Ding J, Huang J. Recent advances on anion-derived sei for fast-charging and stable lithium batteries. *EM* 2021. DOI
237. Zeng X, Mao J, Hao J, et al. Electrolyte design for in situ construction of highly Zn^{2+} -conductive solid electrolyte interphase to enable high-performance aqueous Zn-ion batteries under practical conditions. *Adv Mater* 2021;33:e2007416. DOI PubMed
238. Li D, Cao L, Deng T, Liu S, Wang C. Design of a solid electrolyte interphase for aqueous Zn batteries. *Angew Chem Int Ed Engl*

- 2021;60:13035-41. DOI PubMed
239. Chu Y, Zhang S, Wu S, Hu Z, Cui G, Luo J. In situ built interphase with high interface energy and fast kinetics for high performance Zn metal anodes. *Energy Environ Sci* 2021;14:3609-20. DOI
240. Otani T, Fukunaka Y, Homma T. Effect of lead and tin additives on surface morphology evolution of electrodeposited zinc. *Electrochimica Acta* 2017;242:364-72. DOI
241. Cao L, Li D, Soto FA, et al. Highly reversible aqueous zinc batteries enabled by zincophilic-zincophobic interfacial layers and interrupted hydrogen-bond electrolytes. *Angew Chem Int Ed Engl* 2021;60:18845-51. DOI PubMed
242. Liu Z, Ren J, Wang F, et al. Tuning surface energy of Zn anodes via Sn heteroatom doping enabled by a codeposition for ultralong life span dendrite-free aqueous Zn-ion batteries. *ACS Appl Mater Interfaces* 2021;13:27085-95. DOI PubMed
243. Ouyang K, Ma D, Zhao N, et al. A new insight into ultrastable Zn metal batteries enabled by in situ built multifunctional metallic interphase. *Adv Funct Materials* 2022;32:2109749. DOI
244. Hao J, Yuan L, Ye C, et al. Boosting zinc electrode reversibility in aqueous electrolytes by using low-cost antisolvents. *Angew Chem Int Ed Engl* 2021;60:7366-75. DOI PubMed
245. Zhang Y, Zhu M, Wu K, et al. An in-depth insight of a highly reversible and dendrite-free Zn metal anode in an hybrid electrolyte. *J Mater Chem A* 2021;9:4253-61. DOI
246. Qin R, Wang Y, Zhang M, et al. Tuning Zn²⁺ coordination environment to suppress dendrite formation for high-performance Zn-ion batteries. *Nano Energy* 2021;80:105478. DOI
247. Li F, Yu L, Hu Q, et al. Fabricating low-temperature-tolerant and durable Zn-ion capacitors via modulation of co-solvent molecular interaction and cation solvation. *Sci China Mater* 2021;64:1609-20. DOI
248. Xu W, Zhao K, Huo W, et al. Diethyl ether as self-healing electrolyte additive enabled long-life rechargeable aqueous zinc ion batteries. *Nano Energy* 2019;62:275-81. DOI
249. Cui J, Liu X, Xie Y, et al. Improved electrochemical reversibility of Zn plating/stripping: a promising approach to suppress water-induced issues through the formation of H-bonding. *Mater Today Energy* 2020;18:100563. DOI
250. Feng R, Chi X, Qiu Q, et al. Cyclic ether-water hybrid electrolyte-guided dendrite-free lamellar zinc deposition by tuning the solvation structure for high-performance aqueous zinc-ion batteries. *ACS Appl Mater Interfaces* 2021;13:40638-47. DOI PubMed
251. Chen S, Nian Q, Zheng L, et al. Highly reversible aqueous zinc metal batteries enabled by fluorinated interphases in localized high concentration electrolytes. *J Mater Chem A* 2021;9:22347-52. DOI
252. Du H, Wang K, Sun T, et al. Improving zinc anode reversibility by hydrogen bond in hybrid aqueous electrolyte. *Chem Eng J* 2022;427:131705. DOI
253. Sun P, Ma L, Zhou W, et al. Simultaneous regulation on solvation shell and electrode interface for dendrite-free Zn ion batteries achieved by a low-cost glucose additive. *Angew Chem Int Ed Engl* 2021;60:18247-55. DOI PubMed
254. Qiu M, Ma L, Sun P, Wang Z, Cui G, Mai W. Manipulating Interfacial stability via absorption-competition mechanism for long-lifespan Zn anode. *Nanomicro Lett* 2021;14:31. DOI PubMed PMC
255. Dong Y, Miao L, Ma G, et al. Non-concentrated aqueous electrolytes with organic solvent additives for stable zinc batteries. *Chem Sci* 2021;12:5843-52. DOI PubMed PMC
256. Liu S, Mao J, Pang WK, et al. Tuning the electrolyte solvation structure to suppress cathode dissolution, water reactivity, and Zn dendrite growth in zinc-ion batteries. *Adv Funct Mater* 2021;31:2104281. DOI
257. Lu H, Zhang X, Luo M, et al. Amino acid-induced interface charge engineering enables highly reversible Zn anode. *Adv Funct Mater* 2021;31:2103514. DOI
258. Zhang Q, Luan J, Fu L, et al. The three-dimensional dendrite-free zinc anode on a copper mesh with a zinc-oriented polyacrylamide electrolyte additive. *Angew Chem Int Ed Engl* 2019;58:15841-7. DOI PubMed
259. Yan M, Dong N, Zhao X, Sun Y, Pan H. Tailoring the stability and kinetics of Zn anodes through trace organic polymer additives in dilute aqueous electrolyte. *ACS Energy Lett* 2021;6:3236-43. DOI
260. Hao J, Long J, Li B, et al. Toward high-performance hybrid Zn-based batteries via deeply understanding their mechanism and using electrolyte additive. *Adv Funct Mater* 2019;29:1903605. DOI
261. Bayaguud A, Luo X, Fu Y, Zhu C. Cationic surfactant-type electrolyte additive enables three-dimensional dendrite-free zinc anode for stable zinc-ion batteries. *ACS Energy Lett* 2020;5:3012-20. DOI
262. Zhang Q, Ma Y, Lu Y, et al. Designing anion-type water-free Zn²⁺ solvation structure for robust Zn metal anode. *Angew Chem Int Ed Engl* 2021;60:23357-64. DOI PubMed
263. Zhang S, Hao J, Luo D, et al. Dual-function electrolyte additive for highly reversible Zn anode. *Adv Energy Mater* 2021;11:2102010. DOI
264. Xi M, Liu Z, Ding J, Cheng W, Jia D, Lin H. Saccharin anion acts as a "traffic assistant" of Zn²⁺ to achieve a long-life and dendritic-free zinc plate anode. *ACS Appl Mater Interfaces* 2021;13:29631-40. DOI PubMed
265. Wang N, Zhai S, Ma Y, et al. Tridentate citrate chelation towards stable fiber zinc-polypyrrole battery with hybrid mechanism. *Energy Stor Mater* 2021;43:585-94. DOI
266. Qian L, Yao W, Yao R, et al. Cations coordination-regulated reversibility enhancement for aqueous Zn-ion battery. *Adv Funct Mater* 2021;31:2105736. DOI
267. Chen Z, Chen H, Che Y, et al. Arginine cations inhibiting charge accumulation of dendrites and boosting Zn metal reversibility in aqueous rechargeable batteries. *ACS Sustainable Chem Eng* 2021;9:6855-63. DOI

268. Zhang L, Miao L, Xin W, Peng H, Yan Z, Zhu Z. Engineering zincophilic sites on Zn surface via plant extract additives for dendrite-free Zn anode. *Energy Storage Materials* 2022;44:408-15. DOI
269. Sun KE, Hoang TK, Doan TN, et al. Suppression of dendrite formation and corrosion on zinc anode of secondary aqueous batteries. *ACS Appl Mater Interfaces* 2017;9:9681-7. DOI PubMed
270. Guan K, Tao L, Yang R, et al. Anti-corrosion for reversible zinc anode via a hydrophobic interface in aqueous zinc batteries. *Adv Energy Mater* 2022;12:2103557. DOI
271. Yao R, Qian L, Sui Y, et al. A versatile cation additive enabled highly reversible zinc metal anode. *Adv Energy Mater* 2022;12:2102780. DOI
272. Li R, Li M, Chao Y, et al. Hexaoxacyclooctadecane induced interfacial engineering to achieve dendrite-free Zn ion batteries. *Energy Stor Mater* 2022;46:605-12. DOI
273. Li C, Kingsbury R, Zhou L, Shyamsunder A, Persson KA, Nazar LF. Tuning the solvation structure in aqueous zinc batteries to maximize Zn-ion intercalation and optimize dendrite-free zinc plating. *ACS Energy Lett* 2022;7:533-40. DOI
274. Huang Z, Wang T, Li X, et al. Small-dipole-molecule-containing electrolytes for high-voltage aqueous rechargeable batteries. *Adv Mater* 2022;34:e2106180. DOI PubMed
275. Hou Z, Lu Z, Chen Q, Zhang B. Realizing wide-temperature Zn metal anodes through concurrent interface stability regulation and solvation structure modulation. *Energy Stor Mater* 2021;42:517-25. DOI
276. Cao L, Li D, Pollard T, et al. Fluorinated interphase enables reversible aqueous zinc battery chemistries. *Nat Nanotechnol* 2021;16:902-10. DOI PubMed
277. Zeng X, Xie K, Liu S, et al. Bio-inspired design of an. *in situ* ;14:5947-57. DOI
278. Ma L, Pollard TP, Zhang Y, et al. Functionalized phosphonium cations enable zinc metal reversibility in aqueous electrolytes. *Angew Chem Int Ed Engl* 2021;60:12438-45. DOI PubMed
279. Feng D, Cao F, Hou L, Li T, Jiao Y, Wu P. Immunizing aqueous Zn batteries against dendrite formation and side reactions at various temperatures via electrolyte additives. *Small* 2021;17:e2103195. DOI PubMed
280. Cao L, Li D, Hu E, et al. Solvation structure design for aqueous Zn metal batteries. *J Am Chem Soc* 2020;142:21404-9. DOI PubMed
281. Ballesteros J, Diaz-arista P, Meas Y, Ortega R, Trejo G. Zinc electrodeposition in the presence of polyethylene glycol 20000. *Electrochimica Acta* 2007;52:3686-96. DOI
282. Mitha A, Yazdi AZ, Ahmed M, Chen P. Surface adsorption of polyethylene glycol to suppress dendrite formation on zinc anodes in rechargeable aqueous batteries. *Chem Electro Chem* 2018;5:2409-18. DOI
283. Cao Z, Zhu X, Gao S, et al. Ultrastable zinc anode by simultaneously manipulating solvation sheath and inducing oriented deposition with PEG stability promoter. *Small* 2022;18:e2103345. DOI PubMed
284. Wu Y, Zhu Z, Shen D, et al. Electrolyte engineering enables stable Zn-ion deposition for long-cycling life aqueous Zn-ion batteries. *Energy Stor Mater* 2022;45:1084-91. DOI
285. Huang S, Zhu J, Tian J, Niu Z. Recent progress in the electrolytes of aqueous zinc-ion batteries. *Chemistry* 2019;25:14480-94. DOI PubMed
286. Zhao J, Sonigara KK, Li J, et al. A smart flexible zinc battery with cooling recovery ability. *Angew Chem Int Ed Engl* 2017;56:7871-5. DOI PubMed
287. Kumar G. Electrochemical characterization of poly(vinylidene fluoride)-zinc triflate gel polymer electrolyte and its application in solid-state zinc batteries. *Solid State Ionics* 2003;160:289-300. DOI
288. Kumar G, Sampath S. Spectroscopic characterization of a gel polymer electrolyte of zinc triflate and polyacrylonitrile. *Polymer* 2004;45:2889-95. DOI
289. Zeng Y, Zhang X, Meng Y, et al. Achieving ultrahigh energy density and long durability in a flexible rechargeable quasi-solid-state Zn-MnO₂ battery. *Adv Mater* 2017;29:1700274. DOI PubMed
290. Li Q, Cui X, Pan Q. Self-healable hydrogel electrolyte toward high-performance and reliable quasi-solid-state Zn-MnO₂ batteries. *ACS Appl Mater Interfaces* 2019;11:38762-70. DOI PubMed
291. Liu J, Long J, Shen Z, et al. A self-healing flexible quasi-solid zinc-ion battery using all-in-one electrodes. *Adv Sci (Weinh)* 2021;8:2004689. DOI PubMed PMC
292. Chen M, Zhou W, Wang A, et al. Anti-freezing flexible aqueous Zn-MnO₂ batteries working at -35 °C enabled by a borax-crosslinked polyvinyl alcohol/glycerol gel electrolyte. *J Mater Chem A* 2020;8:6828-41. DOI
293. Zhou W, Chen J, Chen M, et al. An environmentally adaptive quasi-solid-state zinc-ion battery based on magnesium vanadate hydrate with commercial-level mass loading and anti-freezing gel electrolyte. *J Mater Chem A* 2020;8:8397-409. DOI
294. Li H, Liu Z, Liang G, et al. Waterproof and tailorable elastic rechargeable yarn zinc ion batteries by a cross-linked polyacrylamide electrolyte. *ACS Nano* 2018;12:3140-8. DOI PubMed
295. Wang D, Wang L, Liang G, et al. A superior δ-MnO₂ cathode and a self-healing Zn-δ-MnO₂ battery. *ACS Nano* 2019;13:10643-52. DOI PubMed
296. Li H, Han C, Huang Y, et al. An extremely safe and wearable solid-state zinc ion battery based on a hierarchical structured polymer electrolyte. *Energy Environ Sci* 2018;11:941-51. DOI
297. Jin X, Song L, Dai C, et al. A self-healing zinc ion battery under -20 °C. *Energy Stor Mater* 2022;44:517-26. DOI
298. Mo F, Liang G, Meng Q, et al. A flexible rechargeable aqueous zinc manganese-dioxide battery working at -20 °C. *Energy Environ*

- Sci* 2019;12:706-15. DOI
299. Wang Z, Mo F, Ma L, et al. Highly compressible cross-linked polyacrylamide hydrogel-enabled compressible Zn-MnO₂ battery and a flexible battery-sensor system. *ACS Appl Mater Interfaces* 2018;10:44527-34. DOI PubMed
300. Han Q, Chi X, Zhang S, et al. Durable, flexible self-standing hydrogel electrolytes enabling high-safety rechargeable solid-state zinc metal batteries. *J Mater Chem A* 2018;6:23046-54. DOI
301. Huang Y, Liu J, Zhang J, et al. Flexible quasi-solid-state zinc ion batteries enabled by highly conductive carrageenan bio-polymer electrolyte. *RSC Adv* 2019;9:16313-9. DOI
302. Mo F, Chen Z, Liang G, et al. Zwitterionic sulfobetaine hydrogel electrolyte building separated positive/negative ion migration channels for aqueous Zn-MnO₂ batteries with superior rate capabilities. *Adv Energy Mater* 2020;10:2000035. DOI
303. Leng K, Li G, Guo J, et al. A safe polyzwitterionic hydrogel electrolyte for long-life quasi-solid state zinc metal batteries. *Adv Funct Mater* 2020;30:2001317. DOI
304. Wang J, Huang Y, Liu B, et al. Flexible and anti-freezing zinc-ion batteries using a guar-gum/sodium-alginate/ethylene-glycol hydrogel electrolyte. *Energy Storage Materials* 2021;41:599-605. DOI
305. Zhang S, Yu N, Zeng S, et al. An adaptive and stable bio-electrolyte for rechargeable Zn-ion batteries. *J Mater Chem A* 2018;6:12237-43. DOI
306. Chen M, Chen J, Zhou W, Han X, Yao Y, Wong CP. Realizing an all-round hydrogel electrolyte toward environmentally adaptive dendrite-free aqueous Zn-MnO₂ batteries. *Adv Mater* 2021;33:e2007559. DOI PubMed
307. Wei T, Ren Y, Li Z, Zhang X, Ji D, Hu L. Bonding interaction regulation in hydrogel electrolyte enable dendrite-free aqueous zinc-ion batteries from -20 to 60 °C. *Chem Eng J* 2022;434:134646. DOI
308. Tang Y, Liu C, Zhu H, et al. Ion-confinement effect enabled by gel electrolyte for highly reversible dendrite-free zinc metal anode. *Energy Stor Mater* 2020;27:109-16. DOI
309. Cong J, Shen X, Wen Z, et al. Ultra-stable and highly reversible aqueous zinc metal anodes with high preferred orientation deposition achieved by a polyanionic hydrogel electrolyte. *Energy Stor Mater* 2021;35:586-94. DOI
310. Zhang B, Qin L, Fang Y, et al. Tuning Zn²⁺ coordination tunnel by hierarchical gel electrolyte for dendrite-free zinc anode. *Science Bulletin* 2022. DOI
311. Hao Y, Feng D, Hou L, Li T, Jiao Y, Wu P. Gel electrolyte constructing Zn (002) deposition crystal plane toward highly stable Zn anode. *Adv Sci (Weinh)* 2022;9:e2104832. DOI PubMed PMC
312. Xu P, Wang C, Zhao B, Zhou Y, Cheng H. A high-strength and ultra-stable halloysite nanotubes-crosslinked polyacrylamide hydrogel electrolyte for flexible zinc-ion batteries. *J Power Sources* 2021;506:230196. DOI
313. Cao F, Wu B, Li T, Sun S, Jiao Y, Wu P. Mechanoadaptive morphing gel electrolyte enables flexible and fast-charging Zn-ion batteries with outstanding dendrite suppression performance. *Nano Res* 2022;15:2030-9. DOI
314. Nguyen TN, Iranpour B, Cheng E, Madden JDW. Washable and stretchable Zn-MnO₂ rechargeable cell. *Adv Energy Mater* 2022;12:2103148. DOI
315. Liu D, Tang Z, Luo L, et al. Self-healing solid polymer electrolyte with high ion conductivity and super stretchability for all-solid zinc-ion batteries. *ACS Appl Mater Interfaces* 2021;13:36320-9. DOI PubMed
316. Martinolich AJ, Lee C, Lu I, et al. Solid-state divalent ion conduction in ZnPS₃. *Chem Mater* 2019;31:3652-61. DOI
317. Wang Z, Hu J, Han L, et al. A MOF-based single-ion Zn²⁺ solid electrolyte leading to dendrite-free rechargeable Zn batteries. *Nano Energy* 2019;56:92-9. DOI
318. Gao J, Xie X, Liang S, Lu B, Zhou J. Inorganic colloidal electrolyte for highly robust zinc-ion batteries. *Nanomicro Lett* 2021;13:69. DOI PubMed PMC
319. Cao J, Zhang D, Yue Y, et al. Regulating solvation structure to stabilize zinc anode by fastening the free water molecules with an inorganic colloidal electrolyte. *Nano Energy* 2022;93:106839. DOI
320. Xing Z, Xu G, Xie X, et al. Highly reversible zinc-ion battery enabled by suppressing vanadium dissolution through inorganic Zn²⁺ conductor electrolyte. *Nano Energy* 2021;90:106621. DOI
321. Johnsi M, Suthanthiraraj SA. Compositional effect of ZrO₂ nanofillers on a PVDF-co-HFP based polymer electrolyte system for solid state zinc batteries. *Chin J Polym Sci* 2016;34:332-43. DOI
322. Zhao Z, Wang J, Lv Z, et al. In-situ formed all-amorphous poly (ethylene oxide)-based electrolytes enabling solid-state Zn electrochemistry. *Chem Eng J* 2021;417:128096. DOI
323. Johnsi M, Suthanthiraraj SA. Preparation, zinc ion transport properties, and battery application based on poly(vinylidene fluoride-. *co* ;27:877-85. DOI
324. Pucic I, Turkovic A. Radiation modification of (PEO)ZnCl polyelectrolyte and nanocomposite. *Solid State Ionics* 2005;176:1797-800. DOI
325. Nancy AC, Suthanthiraraj SA. Effect of Al₂O₃ nanofiller on the electrical, thermal and structural properties of PEO:PPG based nanocomposite polymer electrolyte. *Ionics* 2017;23:1439-49. DOI
326. Chen Z, Li X, Wang D, et al. Grafted mxene/polymer electrolyte for high performance solid zinc batteries with enhanced shelf life at low/high temperatures. *Energy Environ Sci* 2021;14:3492-501. DOI
327. Karan S, Sahu TB, Sahu M, Mahipal YK, Agrawal RC. Characterization of ion transport property in hot-press cast solid polymer electrolyte (SPE) films: [PEO: Zn(CF₃SO₃)₂]. *Ionics* 2017;23:2721-6. DOI
328. Liu J, Khanam Z, Muchakayala R, Song S. Fabrication and characterization of Zn-ion-conducting solid polymer electrolyte films

- based on PVdF-HFP/Zn(Tf)₂ complex system. *J Mater Sci: Mater Electron* 2020;31:6160-73. DOI
329. Qiu H, Hu R, Du X, et al. Eutectic crystallization activates solid-state zinc-ion conduction. *Angew Chem Int Ed Engl* 2022;61:e202113086. DOI PubMed
330. Adams BD, Zheng J, Ren X, Xu W, Zhang J. Accurate determination of coulombic efficiency for lithium metal anodes and lithium metal batteries. *Adv Energy Mater* 2018;8:1702097. DOI
331. Xiao J, Li Q, Bi Y, et al. Understanding and applying coulombic efficiency in lithium metal batteries. *Nat Energy* 2020;5:561-8. DOI
332. Ma L, Schroeder MA, Pollard TP, et al. Critical factors dictating reversibility of the zinc metal anode. *Energy Environ Mater* 2020;3:516-21. DOI
333. Ma L, Schroeder MA, Borodin O, et al. Realizing high zinc reversibility in rechargeable batteries. *Nat Energy* 2020;5:743-9. DOI